

Master Thesis

TVVR 10/5014

Coastal Erosion on Majuro Atoll, Marshall Islands

With special regard to sea-level rise



Tai Huang
Henrik Rapp

Avdelningen för Teknisk Vattenresurslära

ISRN LUTVDG/TVVR-10/5014

Division of Water Resources Engineering
Department of Building and Environmental Technology
Lund University

Coastal Erosion on Majuro Atoll, Marshall Islands

With special regard to sea-level rise

Tai Huang
Henrik Rapp

Supervisor
Professor Magnus Larson

Examinator
Professor Hans Hanson



LUNDS TEKNISKA HÖGSKOLA

Lunds universitet

Lund University

Faculty of Engineering, LTH

Departments of Earth and Water Engineering

This study has been carried out within the framework of the Minor Field Studies (MFS) Scholarship Programme, which is funded by the Swedish International Development Cooperation Agency, Sida.

The MFS Scholarship Programme offers Swedish university students an opportunity to carry out two months' field work in a developing country resulting in a graduation thesis work, a Master's dissertation or a similar in-depth study. These studies are primarily conducted within subject areas that are important from an international development perspective and in a country supported by Swedish international development assistance.

The main purpose of the MFS Programme is to enhance Swedish university students' knowledge and understanding of developing countries and their problems. An MFS should provide the student with initial experience of conditions in such a country. A further purpose is to widen the human resource base for recruitment into international co-operation. Further information can be reached at the following internet address: <http://www.tg.lth.se/mfs>.

The responsibility for the accuracy of the information presented in this MFS report rests entirely with the authors and their supervisors.

Gerhard Barmen
Local MFS Programme Officer

Acknowledgements

First of all, we would like to thank SIDA and the MFS committee at LTH who granted us the MFS scholarship, which made it possible for us to go to Majuro and write this thesis. We would also like to give thanks to Professor Yokoki and his colleagues for welcoming us into their research group and for all the help, support and guidance we received on Majuro. To Mr. John Bungitak and the staff at the Majuro EPA office, thank you for letting us use your office and for all your efforts in helping us in any way you could. A special thanks goes to Majuro's EPA Coastal Management Advisor Michael Honeth and his family for their hospitality and kindness, and for a friendship that will not be forgotten. To Nettie and Danny and their family, who rented us the small house by the ocean, thank you for taking us in with open arms and treating us as one of your own, and for feeding us all kinds of strange things. To our examiner and head of the Water Resources Engineering Division at LTH, Professor Hans Hanson, thank you for always taking time to help us when we needed it. And a very special thanks to our thesis supervisor Professor Magnus Larson, who presented the idea of a thesis work on Majuro in the first place. Thank you Magnus, for being there every step of the way and helping us with both big and small matters. We are truly grateful for everything you have done for us. Last but not least we would like to thank our friends and families for their support throughout our studies.

Abstract

The Republic of the Marshall Islands is a nation consisting of small coral atolls located in the Pacific Ocean. It is a nation currently listed as a developing country according to the Organization for Economic Cooperation and Development. The Marshall Islands have through history been colonized by Spain, Germany and Japan, and was later during the World War II claimed by the United States. The current population on the Marshall Islands are 60 000 and about half of the population is residing on Majuro, the capital island. Majuro is also the most developed atoll in the Marshall Islands.

Development and increasing population growth on Majuro has brought attention to the coastal problems Majuro is currently facing. Coastal erosion and sea-level rise have become a real and visible threat. Sandy beaches on Majuro are no longer common on the island and seawalls are being built more frequently.

In the IPCC (the Intergovernmental Panel on Climate Change) Fourth Assessment report 2007, small islands are mentioned as particularly sensitive to the effects of climate change, sea-level rise and extreme events. The characteristics of small islands, such as physical size, proneness to natural disasters and low adaptive capacity, make them especially vulnerable to climate change.

To calculate the coastal erosion on Majuro, the first step was to identify and understand different coastal processes. Two types of sediment transport have been analyzed in the thesis, longshore sediment transport and cross-shore sediment transport (dune/berm impact). The longshore sediment transport calculation is based on a wave climate in the lagoon developed from wind data taken from Majuro Sea Level Station. Waves from the ocean side have also been included in the calculations. The results for waves in the lagoon show a sediment transport direction going from east to west, with exception for the most western point on the island. The sediment transport for waves in the lagoon is in the range of -6 000 to 36 500 m³/year (negative means transport from east to west) along the south and west coastline. For ocean side waves the sediment transport range from -66 000 to 105 000 m³/year along affected coastline stretches. Waves from the ocean side reach only some parts of the coastline but show a large impact on the sediment transport along those stretches. A detailed future scenario for the longshore sediment transport was not investigated due to the complexity of the calculations and high uncertainties regarding future wind conditions. However, 10% increase in wind speed yielded 25% increase in sediment transport, which shows the potential impact of a climate change.

The rate of erosion from dune/berm impact was calculated using beach profile measurements performed by SOPAC (Pacific Islands Applied Geoscience Commission) and Professor Yokoki and his colleagues between 1997 and 2009, and the wave climate in the lagoon. The dune/berm impact is also dependent on sea level, which is simulated by using three different sea-level rise scenarios, 0.25m, 0.44m and 0.76m by the year 2100. The third scenario, however, is assumed to have an exponential sea-level rise while the first two are assumed to be linear. The results show that an estimated 32m (32m is chosen due to limitations in the profile measurements) of erosion inland will occur within 70-80 years for the first scenario and 50-60 years for both the second and the third scenario. In the latter half of the

simulation period between 2050-2100, the erosion for the third scenario becomes extremely large because of the exponential increase in sea-level rise.

The risk of overtopping in the Majuro city center in the eastern part of the island has also been investigated in combination with a possible sea-level rise. Statistical analysis based on current wave conditions show that for an increase of 0.2 m in sea level the risk of overtopping will increase 3.5 times. For a 0.4 m sea level rise the risk will increase by 8.5 and for 0.6m the risk increases 15 times.

Climate change and sea-level rise is a multilateral threat for the coastal areas of Majuro. Though coastal management and awareness programs are present on the island it is hard to ignore the fact that Majuro is facing an uncertain future.

Table of content

1	INTRODUCTION	1
1.1	BACKGROUND.....	1
1.2	OBJECTIVES	1
1.3	METHOD	2
2	MAJURO ATOLL, THE REPUBLIC OF THE MARSHALL ISLANDS	3
2.1	AREA DESCRIPTION	3
2.2	HISTORY	5
2.3	GEOLOGY.....	6
2.3.1	<i>Topography Majuro</i>	7
2.4	PROBLEMS IN COASTAL AREAS	7
3	CLIMATE AND SEA-LEVEL RISE ON MAJURO	8
3.1	REGIONAL OCEANOGRAPHY	8
3.2	MAJURO SEA LEVELS	8
3.3	CLIMATE CHANGE	8
3.3.1	<i>The Intergovernmental Panel on Climate Change (IPCC)</i>	8
3.3.2	<i>Small islands</i>	9
4	COASTAL PROCESSES ON MAJURO	10
4.1	CAUSES OF COASTAL EROSION	10
4.1.1	<i>Natural causes</i>	10
4.1.2	<i>Man-induced causes</i>	11
4.1.3	<i>Possible causes of coastal erosion on Majuro</i>	13
4.2	WAVES.....	14
4.2.1	<i>Wave types</i>	14
4.2.2	<i>Wind-generated waves</i>	15
4.2.3	<i>Wave climate Majuro</i>	15
4.3	WAVE TRANSFORMATION.....	16
4.3.1	<i>Shoaling</i>	16
4.3.2	<i>Breaking waves</i>	16
4.3.3	<i>Refraction</i>	16
4.3.4	<i>Diffraction</i>	17
4.3.5	<i>Diffraction in Majuro lagoon</i>	17
4.3.6	<i>Diffraction limitations and assumptions</i>	17
4.4	LONGSHORE SEDIMENT TRANSPORT (LST)	21
4.4.1	<i>Longshore sediment transport processes</i>	21
4.4.2	<i>Direction and magnitude of longshore sediment transport</i>	22
4.5	PREDICTING POTENTIAL LONGSHORE SEDIMENT TRANSPORT ON MAJURO	22
4.6	WAVE RUNUP AND DUNE/BERM IMPACT	24
4.6.1	<i>Wave runup on Majuro</i>	24
4.6.2	<i>Dune and berm erosion on Majuro</i>	26
4.7	OCEAN-SIDE OVERTOPPING ON MAJURO (DUD)	27
4.7.1	<i>Wave set-down and set-up</i>	28

5	FUTURE SEA-LEVEL RISE SCENARIOS	31
5.1	CHOSEN SEA-LEVEL RISE SCENARIOS.....	31
5.1.1	<i>Scenario 1</i>	31
5.1.2	<i>Scenario 2</i>	32
5.1.3	<i>Scenario 3</i>	32
5.2	OVERTOPPING DUD	33
6	RESULTS.....	34
6.1	LONGSHORE SEDIMENT TRANSPORT BY DIFFRACTION	34
6.2	LONGSHORE SEDIMENT TRANSPORT BY LOCAL WAVES	35
6.2.1	<i>Future sediment transport</i>	37
6.3	RUNUP AND DUNE/BERM IMPACT FOR FUTURE SCENARIOS	37
6.3.1	<i>No sea-level rise</i>	38
6.3.2	<i>Sea-level rise scenarios</i>	38
6.4	OVERTOPPING ON DUD	41
7	DISCUSSION	42
7.1	LONGSHORE SEDIMENT TRANSPORT ON MAJURO	42
7.2	WAVE RUNUP AND DUNE/BERM IMPACT	42
7.3	SEA LEVELS AND FUTURE SCENARIOS.....	43
7.4	TOPOGRAPHY	43
7.5	OVERTOPPING	45
8	CONCLUSIONS.....	46
9	REFERENCES.....	47
	APPENDIX I – ABBREVIATIONS	49
	APPENDIX II – COMPUTING WAVE CLIMATE IN THE LAGOON FROM WIND DATA.....	50
	APPENDIX III – CALCULATIONS OF LONGSHORE SEDIMENT TRANSPORT RATE.....	51
	APPENDIX IV – PROFILES AT LAURA	53
	APPENDIX V – WIND DISTRIBUTION AT MAJURO, MARSHALL ISLANDS (GLOSS)	58
	APPENDIX VI – US NAVAL CHART OF MAJURO FROM 1944	59
	APPENDIX VII – SEDIMENT TRANSPORT AS A RESULT OF DIFFRACTION	60
	APPENDIX VIII – EROSION SCENARIOS WITH REGARD TO SEA-LEVEL RISE.....	61
	APPENDIX IX – TABULAR SIGNIFICANT WAVE HEIGHT AND MEAN WAVE PERIOD	63
	APPENDIX X – SUMMERY OF KMNI TOTAL WAVES AND SIGNIFICANT WAVE HEIGHTS AT MAJURO.....	64
	APPENDIX XI – INTERVIEWS ON MAJURO AND JALUIT	65

Table of figures

Figure 2.1 Topographical world map. (commons.wikipedia.org)	3
Figure 2.2 Map of the Republic of the Marshall Islands. (mapsharing.org)	4
Figure 2.3 Satellite image of Majuro Atoll. (flashearth.com)	4
Figure 2.4 Aerial photo of Majuro during WWII, 1945. (uakron.edu)	5
Figure 2.5 Relics from WWII found on Jaluit. (H. Rapp)	5
Figure 2.6 Creation of atolls. (dictionary.com)	6
Figure 2.7 Aerial photos of Jaluit and Majuro Atoll. (H. Rapp)	6
Figure 4.1 Example of erosion on Majuro. (H. Rapp)	10
Figure 4.2 Example of sorting of beach sediment on Majuro. (H. Rapp)	11
Figure 4.3 Example of sorting of beach sediment on Jaluit. (H. Rapp)	11
Figure 4.4 Man-induced erosion on Jaluit cause by pier construction. (H. Rapp)	12
Figure 4.5 Reflection of waves on seawalls. (Hanson, 2010)	12
Figure 4.6 Manmade inlet on the southern rim of Majuro. (H. Rapp)	13
Figure 4.7 Example of a combined wave systems. (U.S. Army Corps of Engineers, 2002)	14
Figure 4.8 Different kinds of waves divided in periods. (U.S. Army Corps of Engineers, 2002)	15
Figure 4.9 Waves generated from winds. (Hanson, 2010)	15
Figure 4.10 Example of wave diffraction in a harbor entrance. (Hanson, 2010)	17
Figure 4.11 Wave diffraction pattern developed by US Army Corps. (U.S. Army Corps of Engineers, 2002)	18
Figure 4.12 Waves entering the lagoon openings on northern Majuro. (IKONOS, 2001)	19
Figure 4.13 Diffraction diagram for correction coefficient k' for the openings for 22.5° waves. (IKONOS 2001)	20
Figure 4.14 Diffraction diagram for correction coefficient k' for the small opening for 60° waves. (IKONOS 2001)	20
Figure 4.15 Shoreline sections of 1000 m with normal and diffraction angle. (IKONOS 2001)	21
Figure 4.16 Locations for of sediment transport calculations and directions of the normal. (IKONOS 2001)	23
Figure 4.17 Example of fetch lengths in the lagoon and an insert showing all fetch lengths. (IKONOS 2001)	23
Figure 4.18 Example of eroded beach and beach berm on Majuro. (H. Rapp)	24
Figure 4.20 Beach profile 8 on Laura measured by SOPAC and Yokoki.	25
Figure 4.19 Location of beach profiles measured by SOPAC. (Yokoki 2009)	25
Figure 4.21 Schematic description of berm erosion due to wave impact in the presence of a scarp.	26
Figure 4.22 Overtopping on Majuro (Marshall Island Journal, December 2008)	27
Figure 4.23 Example of wave set-down and wave set-up. (U.S. Army Corps of Engineers, 2002)	28
Figure 4.24 Chosen location for evaluating overtopping on Majuro. (IKONOS 2001)	29
Figure 4.25 Profile of the chosen point on DUD for overtopping evaluation.	30
Figure 5.1 Sea-level rise for Scenario 1.	32
Figure 5.2 Sea-level rise for Scenario 2.	32
Figure 5.3 Sea-level rise for Scenario 3.	33
Figure 5.4 Average sea level every 10 years in Scenario 3.	33
Figure 6.1 Sediment transport direction for incoming waves at 22.5°. (IKONOS 2001)	34
Figure 6.2 Sediment transport direction for incoming waves at 60°. (IKONOS 2001)	35
Figure 6.3 Sediment transport direction on Majuro Atoll. (IKONOS 2001)	36
Figure 6.4 Potential erosion area for Profile 8.	38
Figure 6.5 Erosion for Scenario 1 at Profile 8.	39
Figure 6.6 Erosion for Scenario 2 at Profile 8.	39
Figure 6.7 Erosion for Scenario 3 at Profile 8.	40
Figure 6.8 Erosion for all 3 scenarios at Profile 8 from 2050-2100.	40
Figure 7.1 Histogram of elevation on the western rim of Majuro together with present and future sea levels.	44

Figure 7.2 Possible erosion scenario on Laura.	44
Figure IV.2 Beach Profile 1 on Laura.	53
Figure IV.1 SOCAP and Yokoki profile measurements on Laura.	53
Figure IV.3 Beach Profile 2 on Laura.	54
Figure IV.4 Beach Profile 3 on Laura.	54
Figure IV.5 Beach Profile 4 on Laura.	55
Figure IV.6 Beach Profile 5 on Laura.	55
Figure IV.7 Beach Profile 6 on Laura.	56
Figure IV.8 Beach Profile 7 on Laura.	56
Figure IV.9 Beach Profile 8 on Laura.	57
Figure IV.10 Beach Profile 9 on Laura.	57
Figure V.1 Wind distribution on Majuro	58
Figure VI.1 US Naval Chart of Majuro from 1944.....	59

1 Introduction

1.1 Background

Sediment transport is a natural occurring phenomenon linking winds and waves, sea level, available sediment and sediment properties, shoreline orientation, and coastal structures. Coastal erosion occurs when a disturbance is introduced in the natural balance causing gradients in the sediment transported from and to the beach, or beach area, by winds and waves generated out at sea. Coastal erosion can be caused by both natural changes, such as shifting of winds and waves, and man-induced changes.

Coastal erosion is a growing concern around the world as coastal areas continue to be an attractive place to live because of urban development, economic growth, and for some, a source of income. Population growth and increasing demands on natural resources puts the already vulnerable coastal areas at great strain. The ever changing interaction between ocean and land has in most urban development not been considered until recent time as the ocean is beginning to impose on manmade infrastructures. For small islands with limited land and resources, this threat is greater than on many other places in the world.

Signs of a change in the climate have in recent years been the subject of many studies. Data analysis has shown a rise in both temperature and sea levels for the past century and also an increase in both the number and intensity of extreme events such as flooding, hurricanes, and tropical storms. These changes have a significant effect on low-lying coastal areas. Rising sea levels contributes to coastal erosion as more land will be exposed to waves and extreme events can in a short period of time threaten the lives of thousands and cause severe damage to infrastructures. Small low-lying islands without proper coastal management and monetary capacity needed to withstand an imposing climate change are in this respect particularly exposed.

Majuro Atoll in the Pacific Ocean is the capital island of the Republic of the Marshall Islands and has 35 000 inhabitants living on a land surface of 49 km². Coastal erosion, increasing population, poverty, and pollution are just a few of the many problems Majuro is currently facing. The complexity of predicting long-term coastal erosion creates a difficult task for decision- and policy makers to maintain a sustainable development in an island environment.

1.2 Objectives

The main objective of this thesis is to estimate the long-term coastal erosion, along with the possible effects climate change might have on the coastlines of Majuro, Marshall Islands. An important goal is to identify and understand the coastal processes on Majuro and to model those to further examine climate change and sea-level rise effects on Majuro. Three future scenarios will be presented to demonstrate the impact on the erosion for different sea-level rise events. Furthermore, discussions and suggestions will be made in an attempt to aid continued coastal management efforts on Majuro.

1.3 Method

In the initial stage, relevant literature, reports, and articles on the Republic of the Marshall Islands, the capital atoll Majuro, and coastal erosion were studied as a preparation for a two-month long site visit on Majuro in June to October, 2009. The site visit was partially financed by SIDA (the Swedish International Development Cooperation Agency) and was made possible through cooperation with a Japanese field expedition headed by Professor Hiromune Yokoki from Ibaraki University. The Japanese provided guidance and assistance as it was their fourth time returning on Majuro for measuring beach profiles and collecting wave data. The beach profiles compiled by Yokoki and the Japanese expedition team are used as a base for examining both present and possible future dune and berm erosion on Majuro.

The site visit provided information and data about the ongoing coastal erosion on the island and also valuable connections with the local Environmental Protection Authority (EPA) and the Japanese expedition team.

Collecting and sorting data from various meteorological and sea level stations in the Pacific Ocean proved to be the key element for modeling the longshore sediment transport. The data was compiled and computed to create a wave climate in the Majuro lagoon. Potential sediment transport in the lagoon was estimated using the wave climate in a new formula for total longshore sediment transport rate developed by Bayram, Larson, and Hanson (2007).

Sea level data was compiled to extract a possible trend line. The current sea-level rise trend at Majuro and two future sea-level rise scenarios by the Delta Committee is used to create three possible scenarios for dune and berm erosion on Majuro. Dune and berm erosion was calculated using a mathematical model developed by Larson, Erikson, and Hanson (2004).

2 Majuro Atoll, the Republic of the Marshall Islands

2.1 Area description

The Republic of the Marshall Islands (RMI) is located in the Pacific Ocean (Figure 2.1) and is one of seven nations located in the South Pacific and belongs to the Oceania sub region of Micronesia. It is the home to 60 000 people. The Marshall Islands consists of 29 atolls with five larger islands and in total 1 225 islands and islets spread out over an area of 1 942 500 km² with a land area of 181 km². The islands create two chains, seen in Figure 2.2, called Ratak to the east (the sunrise chain) and Ralik to the west (the sundown chain). Marshallese and English are the two official languages. The Marshall Islands are according to the Organization for Economic Co-operation and Development (OECD) a developing country and rely heavily on economic aid (RMI Embassy, 2008).

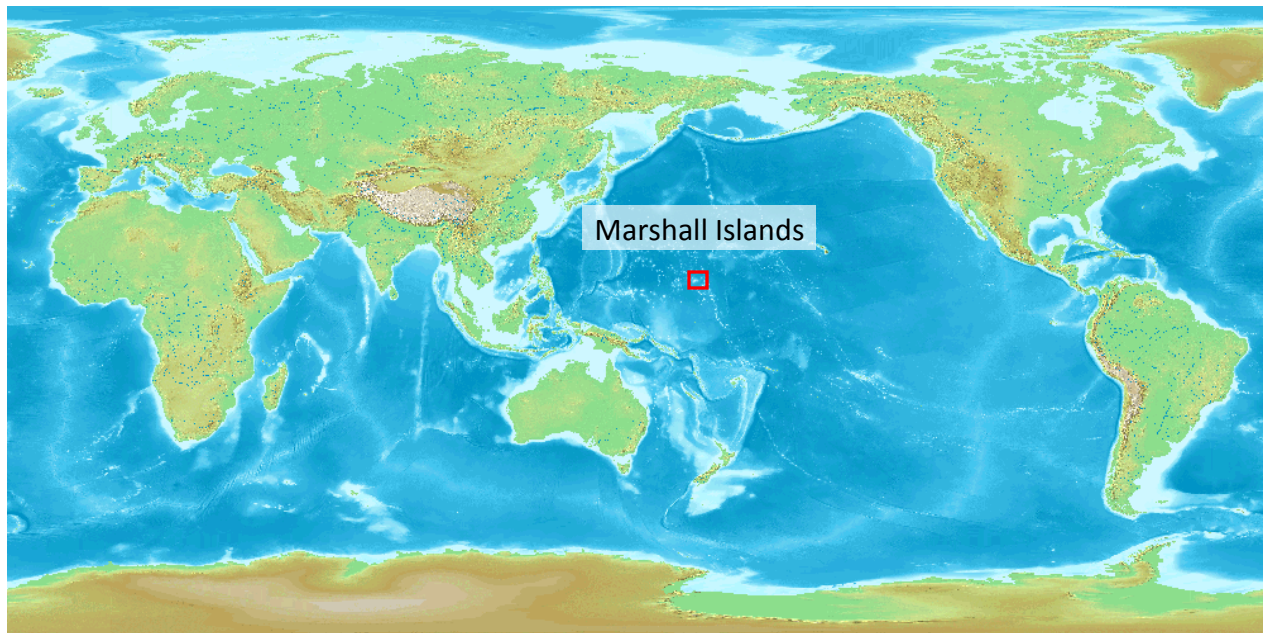


Figure 2.1 Topographical world map. (commons.wikipedia.org)

Majuro Atoll shown in Figure 2.3 has 35 000 inhabitants, which is approximately 50% of the population of the Republic of the Marshall Islands. It is the capital island and the most developed atoll in the country. The Majuro Atoll consists of 64 islets made out of coral reefs surrounding a lagoon. The reefs and islets have a land surface of 49 km² with a mean elevation of 2 m above sea level (Xue, 2001). The lagoon spans 40 km from east to west and 10 km from north to south and covers 344 km² with a maximum depth of 67 m (Xue, 2001). Prevailing trade winds come in from the East-North-East direction. The tide at Majuro Atoll has a daily cycle with a variation in sea level of 1.8 m. Most of the reef is exposed at low tide (Yamano, et al., 2006). The mean temperature is around 27 C° all year-round and the rainy season usually occurs from September to November and the dry season begins in January and ends in April (MIVA, 2005).

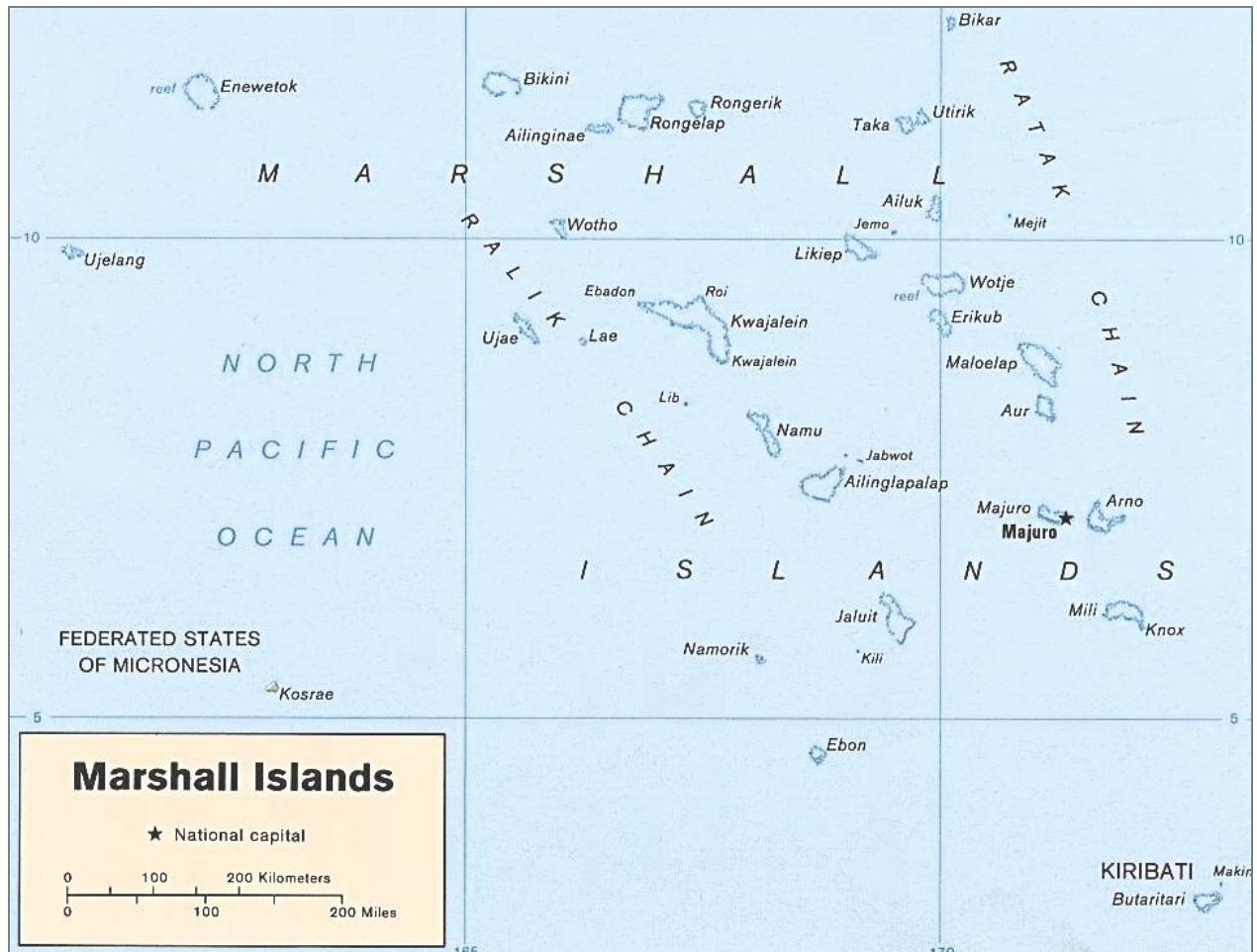


Figure 2.2 Map of the Republic of the Marshall Islands. (mapsharing.org)

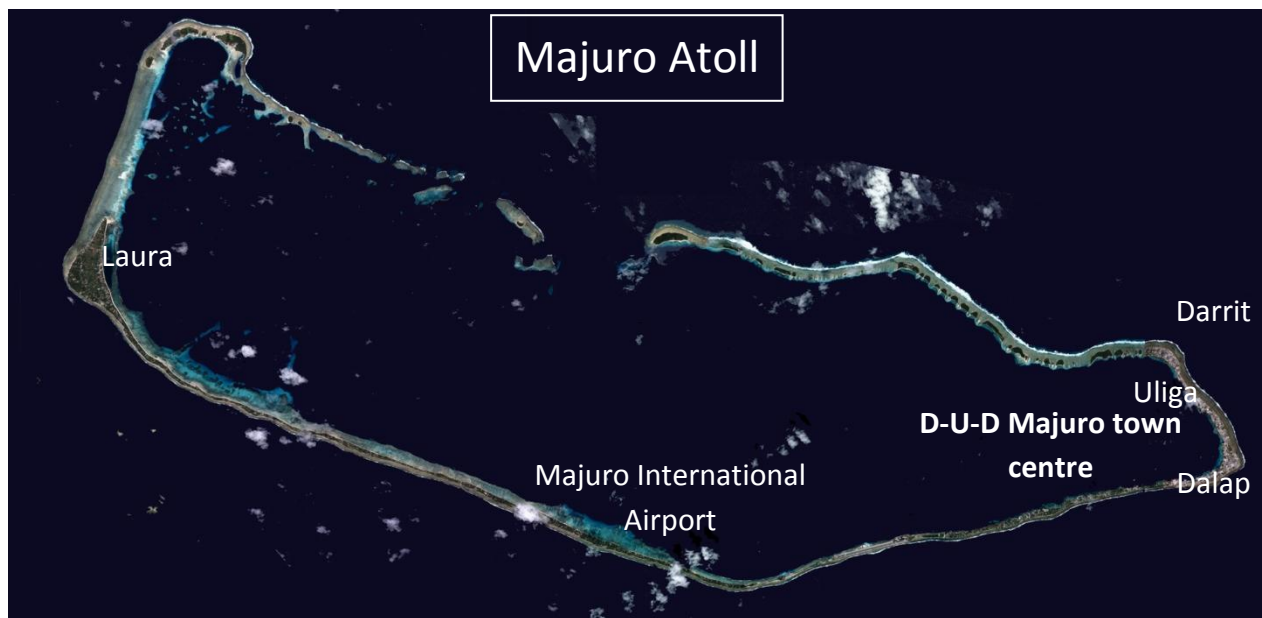


Figure 2.3 Satellite image of Majuro Atoll. (flashearth.com)

2.2 History

It is believed that the Marshall Islands were first populated over 3000 years ago by Polynesian explorers. The Islands have since then had several colonial owners, Spain being the first in the 16th century. The Marshall Islands got its name from the English naval captain William Marshall who sailed through the area in the 18th century. Germans entered the Marshall Islands in the 1850's. A trading post was setup and the Germans settled in. As profits from copra production grew, a dispute arose over territorial and commercial rights in Micronesia, which eventually led the Germans to purchase the islands from Spain in agreement with the native Marshallese chiefs in 1885. Germany held the Marshall Islands as an economic colony but without any means of protection in case of war. When World War I broke out, Japan took military possession of the island in 1914 and eventually lost it to the Americans at the end of the 2nd World War (Figure 2.4). During this time plenty of remnants were scattered all over the islands, some of which are shown in Figure 2.5. RMI became a self-governing state in 1986, with the United States responsible for their security and defenses. The US still provides economic aids for compensation of the nuclear testing done on Bikini and Eniwetok Atoll during the 40's and 50's. US military is still present on Kwajalein Atoll under a lease from the Marshall Islands government, where a US military missile testing range is located. (RMI Embassy, 2008)



Figure 2.4 Aerial photo of Majuro during WWII, 1945. (uakron.edu)



Figure 2.5 Relics from WWII found on Jaluit. (H. Rapp)

2.3 Geology

Atolls such as the ones in the Marshall Islands are believed to have been created from sinking prehistoric volcanoes surrounded by coral reefs (Figure 2.6). As the volcanoes slowly submerged into the ocean the coral reefs kept growing and layering the top surface creating rings of coral atolls seen today (Figure 2.7).

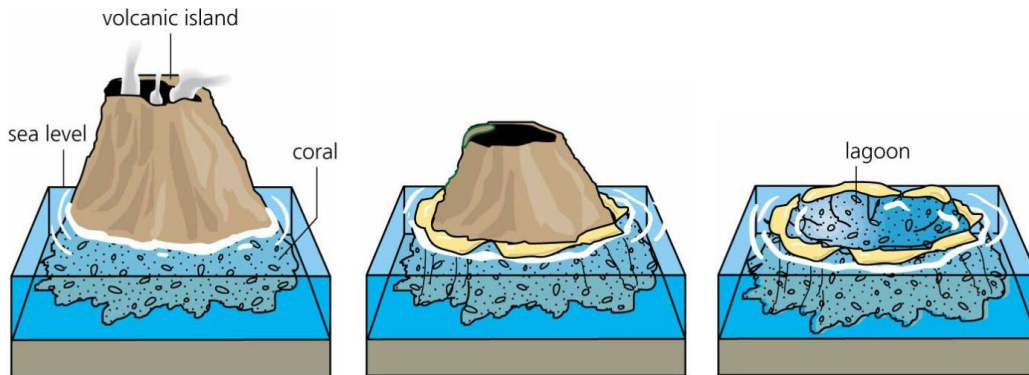


Figure 2.6 Creation of atolls. (dictionary.com)

Solid islands without a lagoon were likely created in the same way, though from smaller peaks. Compared to the atolls around the world the ones of the Marshall Islands are much larger and surrounded by numerous islets seemingly dominant on the windward side. With the help of deep core drilling it has also been determined that the atolls in the Marshall Islands were colonized by terrestrial life merely 3 000-4 000 years ago, which is considered to be extremely young from a geological perspective. Hawaii for example, is believed to have been created in the range of millions of years (The National Biodiversity Team of the Republic of the Marshall Islands, 2000).



Figure 2.7 Aerial photos of Jaluit and Majuro Atoll. (H. Rapp)

A closer look at the composition of coral reefs and atoll foundations shows that the most obvious building block appears to be stony and hard corals. Yet far more marine species which are not immediately apparent plays a vital role in the creation of reefs and atolls. These species, such as loose sediment bits of seashells, sea urchins, calcareous cactus algae etc. serve as fills to the bigger blocks. The major contributor of finer material on Majuro is produced by singled-celled organisms called foraminiferan (SOPAC, 1995). The foraminiferans are tiny grain-like organisms capable to produce their own calcium carbonate shells (The National Biodiversity Team of the Republic of the Marshall Islands, 2000). There are entire beaches in the Marshall Islands made of almost pure foraminiferan shells. Other contributors to fine sediments are the bioeroders, marine animals that feed on coral such as parrotfish and triggerfish.

The coral reef surrounding the Marshall Island Atolls does not only host a vast biodiversity of marine life, but serves also as protection against erosion. A healthy and intact coral reef ecosystem is vital for the island, since the reef reduces the wave energy before the waves hit the shore and causes erosion. Many of the atolls in the Marshall Islands have currently a coral reef ecosystem in excellent condition. In recent years however, the coral reefs have become increasingly threatened by fisheries, climate change and sea-level rise, and increasing urbanization (Beger, et al., 2008).

2.3.1 Topography Majuro

As mentioned before the mean elevation of The Marshall Islands is approximately 2 m above mean sea level. On Majuro most of the field surveys have been performed on Laura, located in the western part of Majuro. One reason for this is that the main groundwater source is located here. In the west part of Majuro the topography is slightly higher than in the rest of Majuro. Although the topography is higher here, Laura only has a mean height of approximately 2.7 m above mean sea level.

2.4 Problems in coastal areas

Majuro continues to develop with increasing population rates and more land protection structures against the ocean are being built. From a coastal management point of view, the effects of coastal structures should to be investigated for the benefit of the whole island, which is often not the case. Seawalls cover the coastlines in the city center in the eastern part of the atoll (DUD area) with almost no exception. The construction of the causeway and airport at the southern rim of the island, along with constructed seawalls, were mentioned by locals as possible sources for the recent accelerated erosion on Majuro. Though permission is needed from the EPA (Environmental Protection Authority) for any costal structures, permissions to build seawalls are in general rather easy to obtain.

One of the more obvious coastal problems on Majuro is the waste management on the island. Majuro Atoll is heavily populated in the DUD area. It is also in the DUD area where most of the accumulated waste is seen in the lagoon. However, currents in the lagoon transport some of the waste along the coast to other parts of the island. Some of the waste is also found on the bottom of the lagoon. Pollution in the form of oil leaks from fishing vessels is also commonly found in lagoon. The pollution causes harm to the biological ecosystem in the ocean and provides an indirect contribution to the coastal erosion because most of the sediment in the area is generated by marine life.

3 Climate and sea-level rise on Majuro

3.1 Regional oceanography

The climate in the Pacific Island region is entirely ocean-dependent and highly linked to the inter-annual warm ocean current that flows along the equator from the date line and south off the coast of Ecuador, also known as El Niño. The phenomenon carries the warm surface water from the tropical Pacific towards South America, along with clouds and rain. The shifting of clouds towards east causes a drought in Indonesia and Australia and brings at same time heavy rain and hurricanes to the central parts of the Pacific. El Niño reoccurs every 4-7 years and lasts for about 12-17 months and is usually recognized by a significant increase in water surface temperatures in a large area of the eastern Pacific (SMHI, 2009).

Changes associated with El Niño will affect the sea level, winds, precipitation, and air and water temperatures in the region. The impact of the 1997/1998 El Niño caused highly noticeable irregularities on Majuro, such as very low sea levels and barometric pressures (MIVA, 2005).

A similar phenomenon named La Niña is also affecting the climate in the Pacific Ocean. La Niña carries cold surface water along the equator in the central and eastern parts of the Pacific in a cycle of 3-4 years. The effects of La Niña are mostly noticeable in the tropical and southern parts of the hemisphere (SMHI, 2009).

Although the Marshall Islands is located in the Pacific typhoon belt, typhoons are considerably rare. A large typhoon in 1918 struck Majuro and caused over 200 casualties. The latest encounter of a devastating cyclone was on the 10th of December 1997, when a typhoon named Paka (MIVA, 2005) hit the islands.

3.2 Majuro sea levels

The Global Sea Level Observation System (GLOSS) has a network of 290 sea level stations around the world, including in Majuro. It is an international program endorsed by the Joint Commission for Oceanography and Marine Meteorology (JCOMM) of the World Meteorological Organization (WMO) and the Intergovernmental Oceanographic Commission (IOC). The Department of Oceanography at the University of Hawaii is the authority undertaking the responsible for the tidal gauge at Majuro. Sea level data from Majuro were collected from two locations spanning from 1968-1999 at the first location and 1994 to present time at the second location. The location change was made when the AusAid-sponsored South Pacific Sea level and Climate Monitoring Project (SPSLCP) installed a SEAFRAME (Sea Level Fine Resolution Acoustic Measuring Equipment) gage at Majuro in 1993 (SPSLCP, 2007). Because of different reference points and precision, the two series should not be used jointly.

3.3 Climate change

3.3.1 The Intergovernmental Panel on Climate Change (IPCC)

United Nations Environment Programme (UNEP) and the World Meteorological Organization (WMO) established in 1989 IPCC, the now leading body for the assessment of climate change. The United Nations goal was to provide governments around the world with a clear scientific view of the situation regarding climate change (IPCC, 2010). The first IPCC Assessment report in 1990 became an eye-opener

to the topic and set in motion the creation of the United Nations Framework Convention on Climate Change (UNFCCC), the key international treaty on reducing global warming and coping with the effects of climate change. IPCC has since then produced Assessment Reports and Special Reports on various climate topics regularly, consisting of scientific reports worldwide (IPCC, 2010).

3.3.2 Small islands

IPCC expresses a concern regarding the particular effects of climate change, sea level rise, and extreme events on small islands. It is believed that the characteristics of small islands (physical size, proneness to natural disasters and climate extremes, low adaptive capacity) make them especially vulnerable to any possible climate change. Small islands in the Pacific also face other contributing factors to their vulnerability, such as rapid population growth and urbanization, limited natural resources and space, socio-economic conditions, political instability and poorly developed infrastructure. Most of the population and infrastructure, such as international airports, roads, and capital cities, in small islands in the Pacific are generally located in coastal areas. Water resources on small islands are also extremely vulnerable to changes and variations in the climate as they are highly dependent on rainfall harvesting and replenishment of scarce fresh water lenses. Reduction in precipitation and saltwater intrusion as a result of severe coastal erosion are just a few possible future impacts resulting from climate change. (Mimura, et al., 2007)

Sea level rise rates in the Pacific calculated from the SEAFRAME stations, using stations with 50 years of data or more, yield an average sea-level-rise of 1.6 mm/year (Mimura, et al., 2007). Yet indications of geographical variations have been found due to non-uniform distribution of temperature, salinity, and changes in ocean circulation.

4 Coastal processes on Majuro

4.1 Causes of coastal erosion

The causes of coastal erosion can be divided into two different types, natural and man-induced erosion.

4.1.1 Natural causes

Sea-level rise

Sea-level rise causes a long-term shift in the position of the coastline. Erosion can be caused by both flooding and beach profile adjustment due to higher water levels (U.S. Army Corps of Engineers, 2002). Examples of heavy erosion on Majuro are shown in Figure 4.1.



Figure 4.1 Example of erosion on Majuro. (H. Rapp)

Storm Waves

Steep waves from storms cause sediment transport from the beach and create temporary bars or shoals. In calm weather some of the sediment will be transported back upon the beach, but in most cases some of the sediment is lost to deeper water (U.S. Army Corps of Engineers, 2002).

Waves and Surge Overwash

Overwash can occur during storms surge and when large swell waves reach land. These phenomena affect the area above the normal beach, transporting sediment out to sea or over the land area and out in the lagoon on the other side (U.S. Army Corps of Engineers, 2002).

Deflation

During hard wind loose sediment can be blown from land out to sea (U.S. Army Corps of Engineers, 2002).

Longshore Sediment Transport

Sediment is transported by currents created from waves breaking at an angle to the shoreline. The currents transport the sediment along the shore. Erosion occurs if there are gradients in the transport, meaning more sediment is transported from an area than to it (U.S. Army Corps of Engineers, 2002).

Sorting of Beach Sediment

The sediment is distributed over the beach profile depending on the size and the hydraulic properties of the sediment together with the forcing. This is a common phenomenon on beaches also seen in The Marshall Islands (Figure 4.2 and 4.3). In general the coarse sediment is transported up on the beach and the finer sediment is transported away from the shoreline and out towards the sea. Because of this sorting fine material eroded from the beach scarp can be transported out to deeper water and in some cases be lost from the beach area.



Figure 4.2 Example of sorting of beach sediment on Majuro. (H. Rapp)



Figure 4.3 Example of sorting of beach sediment on Jaluit. (H. Rapp)

4.1.2 Man-induced causes

Interruption of Sediment Transport

Interruption of longshore sediment transport is probably the most common cause of man-induced erosion. Improvements of channels by dredging and harbor structures capture the sediment and the material is permanently lost from the downdrift beach. Construction of groins, rubble mounds, and seawalls to protect areas from erosion can also disturb the downdrift supply of material. Structures that interrupt longshore transport are typical on The Marshall Islands and an example is shown in Figure 4.4.

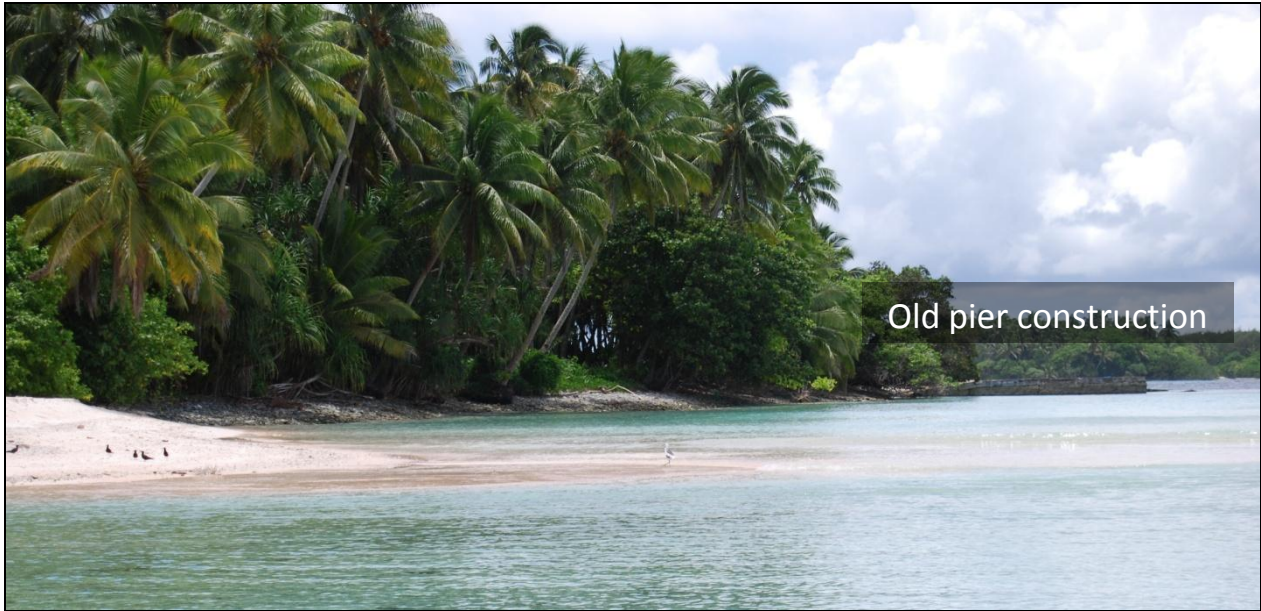


Figure 4.4 Man-induced erosion on Jaluit cause by pier construction. (H. Rapp)

Concentration of Wave Energy on Beaches

Placement of coastal structures like vertical walls in the beach area may increase the energy due to wave reflection from the seawall (Figure 4.5). Thus, areas located in the vicinity of the structure may get exposed to increased forcing because of the reflected waves, resulting in increased erosion of nearby beaches.

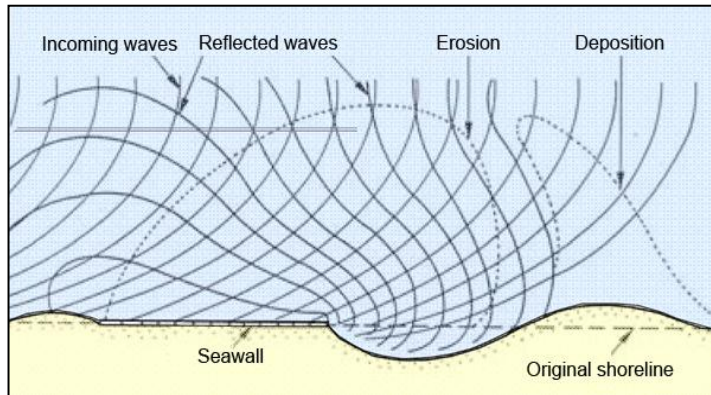


Figure 4.5 Reflection of waves on seawalls. (Hanson, 2010)

Increase in Water Level Variation

Deepening and widening of inlets and navigational channels may affect the tide in a lagoon, as well as allowing larger swell waves to enter. The tide and the swell may expose more of the beach resulting in increased erosion and changes in the beach profiles. These man-made inlets are also common in the Marshall Islands (Figure 4.6).



Figure 4.6 Manmade inlet on the southern rim of Majuro. (H. Rapp)

Change in Natural Coastal Protection

Dredging of the nearshore areas may increase the energy of the waves that reach the beach. Other changes in the natural protection are the leveling of beach dunes, destructions of beach vegetation, paving of back shore areas, and construction of small boat channels. All these changes may increase the potential for erosion and overwash, including the risk of breaching on small islands.

Removal of Material from Beaches

Excavation of beach material to be used for construction, landfills, or recreation is sometimes undertaken. Whatever the purpose, this results in a direct loss of material from the beach.

Sinking of land caused by removal of subsurface resources

Removal of natural resources such as groundwater close to the coastal zone can change the hydrostatic equilibrium affecting the soil structure causing the land to subside.

4.1.3 Possible causes of coastal erosion on Majuro

The above-discussed causes of erosion can all be observed on Majuro. Hard coastal structures, especially seawalls, are likely to be one of the major causes for the recent changes in sediment transport patterns. Sandy beaches are nowadays only found in a few places on Majuro. Material used for constructions is not easily obtained on Majuro and up until recently material has been taken from quarries on both the lagoon and ocean side. Recent studies from SOPAC have shown a worrying increase in the erosion as a result of the dredging, mostly visible on Laura where sandy beaches previously were in abundance. Sand material is also commonly taken from the beach by locals to be used as filling material for various purposes. Educational efforts have been made by EPA by implementing environmental awareness programs and to teach locals about the possible effects of removal of sand material from the beach. Still, sand material remains a scarce and valuable resource, very much available for anyone to take.

4.2 Waves

It is in most cases hard to determine where a specific wave on the open sea starts and ends. The reason is that a wave often consists of a combination of several different waves generated from different places. After a wave is created it may travel hundreds or thousands of kilometers. What may seem to be one wave could in fact be several waves coexisting (Figure 4.7). This phenomenon creates a highly complicated system to describe and model. However, as the waves propagate without any effects from wind they tend to take on sinusoidal shape, which is used in many wave theories. Waves are identified by assessing the wave period, height, and the length of the wave fronts (U.S. Army Corps of Engineers, 2002).

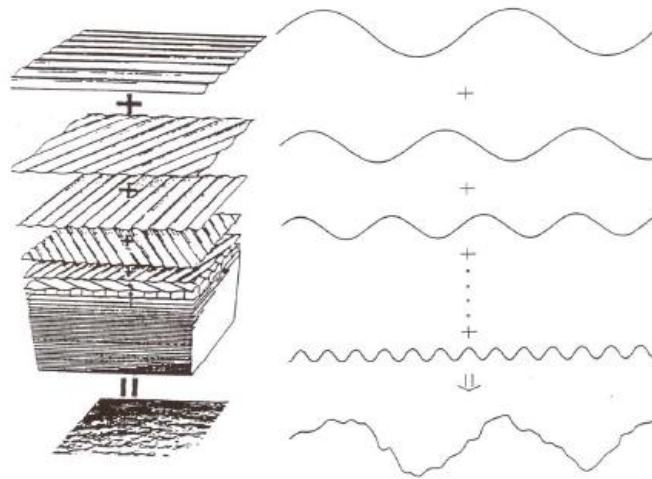


Figure 4.7 Example of a combined wave systems. (U.S. Army Corps of Engineers, 2002)

4.2.1 Wave types

One way to classify waves is by divide them by the wave period (Figure 4.8). The spectrum of wave periods reaches from less than a second to several days. Waves with short periods are the common wind-generated waves and they have the most long-term effects on beaches and coastal structures. Under the category of long-period waves are tsunamis, tides, and storm surges. Tsunamis are caused by sudden events like landslides or earthquakes. Tsunamis are unpredictable and hold a great amount force, but are fortunately not very common. Tides on the other side are common and predictable events caused by the gravitational forces from the sun and moon. Most tides can be calculated with high accuracy. Surges are caused by large bodies of water that is being pushed in front of a storm system. Depending on the magnitude, these forceful events can have a major effect on the shoreline, especially on exposed lowlands (U.S. Army Corps of Engineers, 2002).

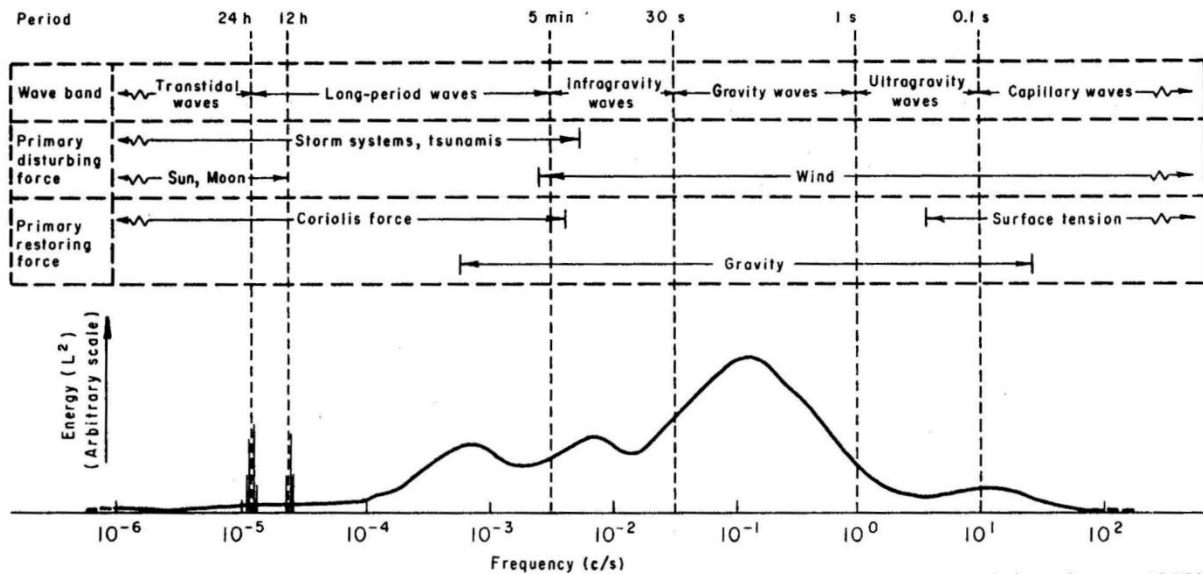


Figure 4.8 Different kinds of waves divided in periods. (U.S. Army Corps of Engineers, 2002)

4.2.2 Wind-generated waves

Wind-generated waves are created by pressure differences and friction between the lower layer of the wind and the water surface (Figure 4.9). As the wind sweeps across the water surface, the friction in the lower layer of the wind slows down, creating a low pressure in the front. When the wind reaches the surface a high pressure is enforced. As the wave takes form, the pressure in front of the wave crest becomes higher than behind the wave and forces the wave to move forward (U.S. Army Corps of Engineers, 2002).

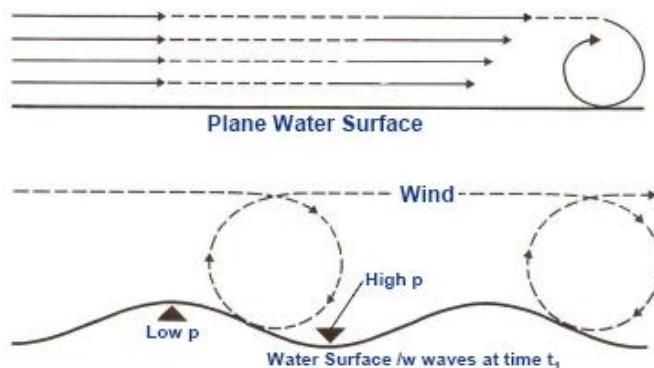


Figure 4.9 Waves generated from winds. (Hanson, 2010)

4.2.3 Wave climate Majuro

The wave climate on Majuro originates from two sources, ocean waves and lagoon waves. The ocean wave climate was calculated by KNMI (The Royal Netherlands Meteorological Institute) based on a combination of observational data using satellites and numerical modeling for the time period January 1971 and December 2000 (KNMI, 2000). The information employed consisted of significant wave height (H_s) and mean wave period (T_m). The wave climate has been divided into groups representing 45-degree sectors. Because there is no time series information available for the ocean waves, a combined analysis of waves and tidal variations was not possible.

Wave climate in the Lagoon was calculated based on hourly wind data measured on the Majuro SEAFRAME station between 1994 and 2009. The wind data series at the SEAFRAME station was chosen due to its higher resolution compared to other available data.

Winds are driven by large-scale pressure gradients in the atmosphere that in turn may push large bodies of water in front of them (U.S. Army Corps of Engineers, 2002). At an elevation of 10 to 100 meter above the ocean it is possible to develop an equation for the vertical variation in wind speed (Appendix II). The wind data from the SEAFRAME station in Majuro is assumed to be measured at 10 m above sea level. By using the adjusted wind speed and direction and use the fetch length as a limiting factor for the maximum wave height, the wave height in the lagoon can be obtained through calculations. However, if equilibrium in the wave height is reached before the full length of the fetch has passed, the maximum wave height is then solely dependent of the wind speed. Adjustments for fully developed waves have been taken in to account. The lagoon is considered to be “deep water”, i.e., a depth/wavelength ratio of ½ prevails in the wave-generation area of the lagoon.

4.3 Wave transformation

4.3.1 Shoaling

In deep water most waves may be characterized by a sinusoidal shape. As they approach shallow water the wave height and wavelength start to change gradually, whereas the period remains constant. The reduction in water depth causes the waves to shoal. Thus, the height and steepness of the waves increase until they become unstable and break.

4.3.2 Breaking waves

When a wave breaks energy will be lost (Komar, 1997). Theoretically, breaking starts when the ratio between the wave height and the depth is 0.78, and if the depth does not change the wave will continue to lose energy until equilibrium is reached. This occurs when the ratio between the wave height and the depth is approximately 0.4. If the wave reenters deep water (e.g., behind a shallow reef), it will go back to its former state having a sinusoidal form with the deep-water wavelength L_0 :

$$L_0 = \frac{g}{2\pi} \cdot T^2 \rightarrow 1,56 \cdot T^2 \quad (4-1)$$

The wave phase speed (C_0) is given by:

$$C_0 = \frac{g}{2\pi} \cdot T \rightarrow 1,56 \cdot T \quad (4-2)$$

Although the speed and wavelength after crossing shallow water and coming into deep water again is the same, the wave height has decreased due to the loss of energy.

4.3.3 Refraction

Refraction occurs when the wave front approach shallow water at an angle that differs from the orientation of the bottom contours. As one end of the wave front reaches shallow water this end will slow down (the wave speed decreases with water depth), whereas the other end will maintain its

original speed. This will force the wave to change direction. Due to this phenomenon a wave will approach more perpendicular to the beach contours even though the offshore wave direction might be more oblique. In coastal hydraulics this phenomenon is a great significance for the magnitude of longshore sediment transport rate.

4.3.4 Diffraction

When a wave front reaches a gap towards a sheltered area, such as a harbor entrance or a small island, the wave will diffract. Thus, when the wave front enters the gap the part of the wave front outside the gap will be blocked. After the obstacle is past, the crest of the wave will propagate out into the lee region because of the water surface slope on the sides (Figure 4.10). Due to this spreading out, the wave height will decrease the further away from the middle of the gap that it gets. For constant water depth, the wave speed and period remains the same and near-circular pattern is created in the lee zone.

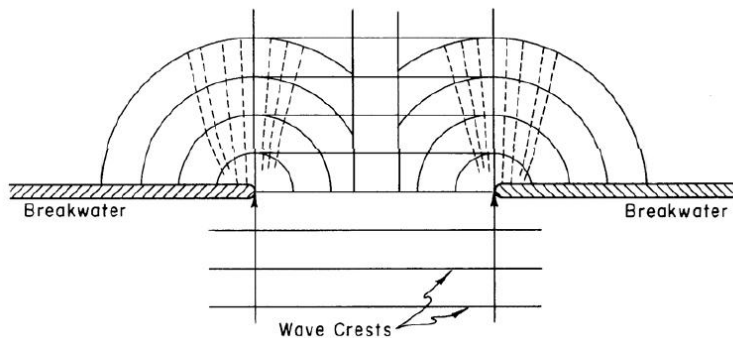


Figure 4.10 Example of wave diffraction in a harbor entrance. (Hanson, 2010)

4.3.5 Diffraction in Majuro lagoon

Majuro atoll has two major openings into the lagoon. These openings are located on the northern rim of the atoll. The largest one is approximately 3 km wide and the smallest one is 1.4 km wide. Most of the ocean side waves approaches from the east, which means that the lagoon is sheltered from some of the waves. Still, approximately 40% of the waves will enter the lagoon. As the waves reach the openings and propagate into the lagoon, the edges will cause a diffraction pattern in the lagoon.

4.3.6 Diffraction limitations and assumptions

As previously discussed, significant ocean wave height and mean period were obtained from the Royal Netherlands Meteorological Institute (KNMI, 2000). The diffraction pattern for the Majuro lagoon straits was adapted from the Shore Protection Manual, U.S. Army Corps of Engineers, 2002 (Figure 4.11). It is assumed that the diffraction at the opening edges are independent as the width exceeds 5 wavelengths in both cases.

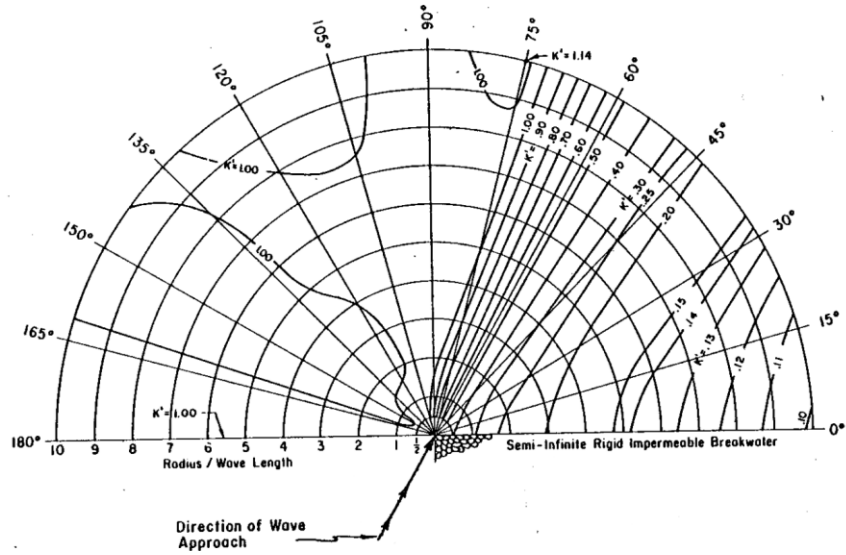


Figure 4.11 Wave diffraction pattern developed by US Army Corps. (U.S. Army Corps of Engineers, 2002)

KNMI/ERA-40 wave atlas is based on observations by ships and weather stations and calibrated with data from deep water buoys on the northern hemisphere. The wave data used in this analysis is based on 1 577 952 values from 1971-2000 at Lon (171,180) Lat (0,9) (Marshall Islands) (KNMI, 2000). The waves were divided in 45 degree sectors with period, height, and number of waves. However, the orientation of the northern openings on Majuro will limit more than half of the total waves from entering the lagoon with the exception of waves from 0-45 and 45-90 degrees. The small amount of waves from NNW 315-360 degrees where neglected and the other directions have no impact on the wave climate in the lagoon due to their direction (**Error! Reference source not found.**).

Table 4.1 KNMI wave direction and quantity.

	NNE	ENE	ESE	SSE	SSW	WSW	WNW	NNW
KMNI approach angle	0-45°	45-90°	90-135°	135-180°	180-225°	225-270°	270-315°	315-360°
% of total waves	18%	38%	33%	8%	1%	0%	0%	2%
Actual approach angle	0-45°	45-75°	90-135°	135-180°	180-225°	225-270°	270-315°	315-360°
% of total waves	18%	25.3%	33%	8%	1%	0%	0%	2%

Waves spanning from 0-45° will enter through both openings on Majuro at a mean wave direction of 22.5° (Figure 4.12). Waves from 45-90° will only enter through the smaller opening and only from 45-75° due to its orientation, meaning only 2/3 the total KMNI waves will entering from ENE (Table 4.1). The 45-75° waves are given a mean wave direction of 60° (Figure 4.12).

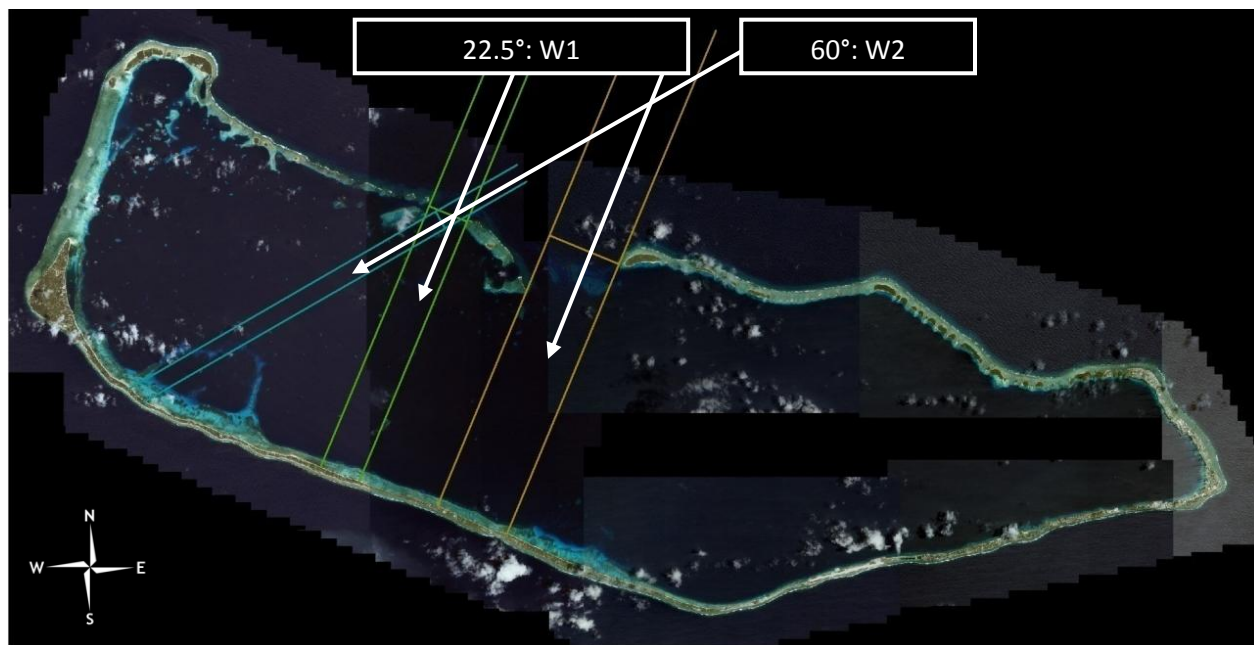


Figure 4.12 Waves entering the lagoon openings on northern Majuro. (IKONOS, 2001)

A U.S. naval sea chart from 1944 (Appendix VI) was used to obtain water depths, whereas the tidal variations and the refraction effect were excluded to simplify the diffraction calculations. In reality the water depth varies locally depending on the reef and tidal changes.

As the waves enter the openings and collide with the shallow reefs surrounding the island, the waves tend to break. There are two different wave angles to consider W1 and W2 (Table 4.2). Based on the water depth, all waves entering the small opening to the west will break and obtain a maximum height of approximately 0.8 m (W1 broken, W2 broken). For the bigger opening, approximately 4.5 % of the W1 waves will not break and travel over the reef into the lagoon (W1 unbroken) and approximately 13.5 % will break and get a maximum height of 1.6 m (W1 broken) (Table 4.2). Once the broken waves pass the reef flat they will re-stabilize and start shoaling and diffracting. The diffraction diagram and coefficients for the two wave angles are shown in Figure 4.13 and Figure 4.14. The reef flat is several times longer than any wavelength obtained from the KMNI data, thus, the breaking wave index is set to 0.4, which corresponds to equilibrium conditions for the breaking process. These corrections were applied to the wave cases W1 and W2.

Table 4.2 Cases for ocean waves entering the lagoon.

Opening	Large (East)		Small (West)	
Water depth (m)	4		2	
Wave case	W1 (broken)	W1 (unbroken)	W1 (broken)	W2 (broken)
Wave Direction	0 - 45	0 - 45	0 - 45	45 - 75
Breaking height	1.6	1.42	0.8	0.8
Approach angle	22.5	22.5	22.5	60
% of actual waves	13.5	4.5	18	25.3

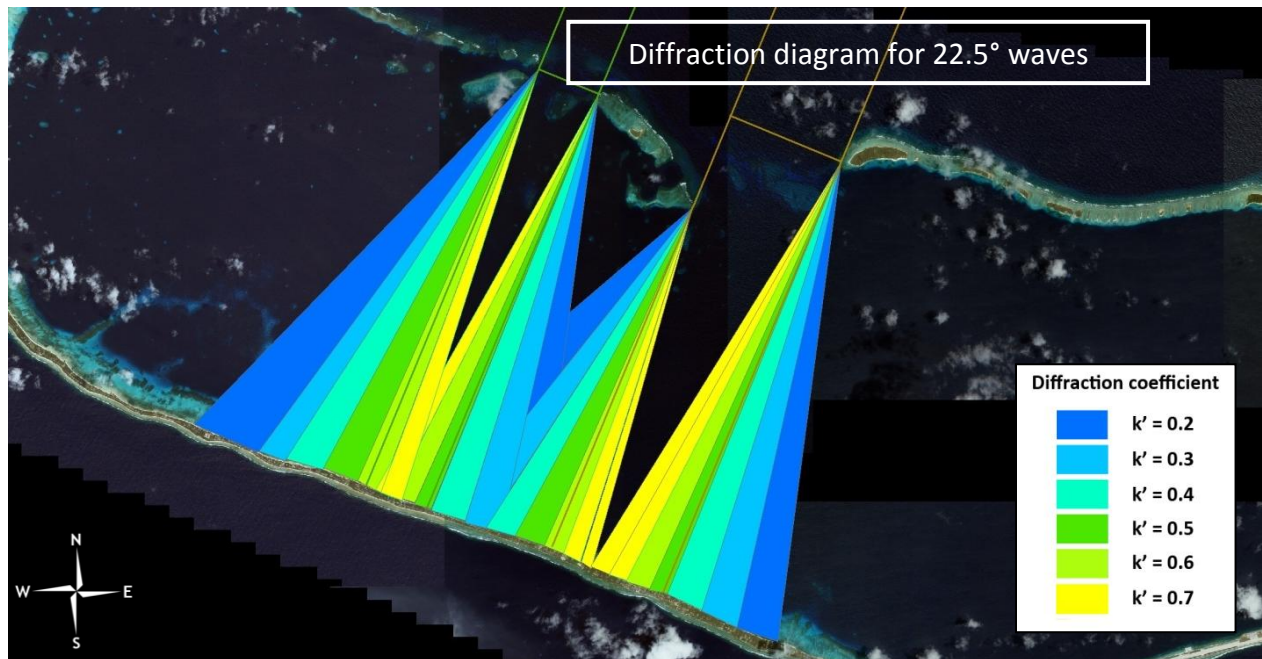


Figure 4.13 Diffraction diagram for correction coefficient k' for the openings for 22.5° waves. (IKONOS 2001)

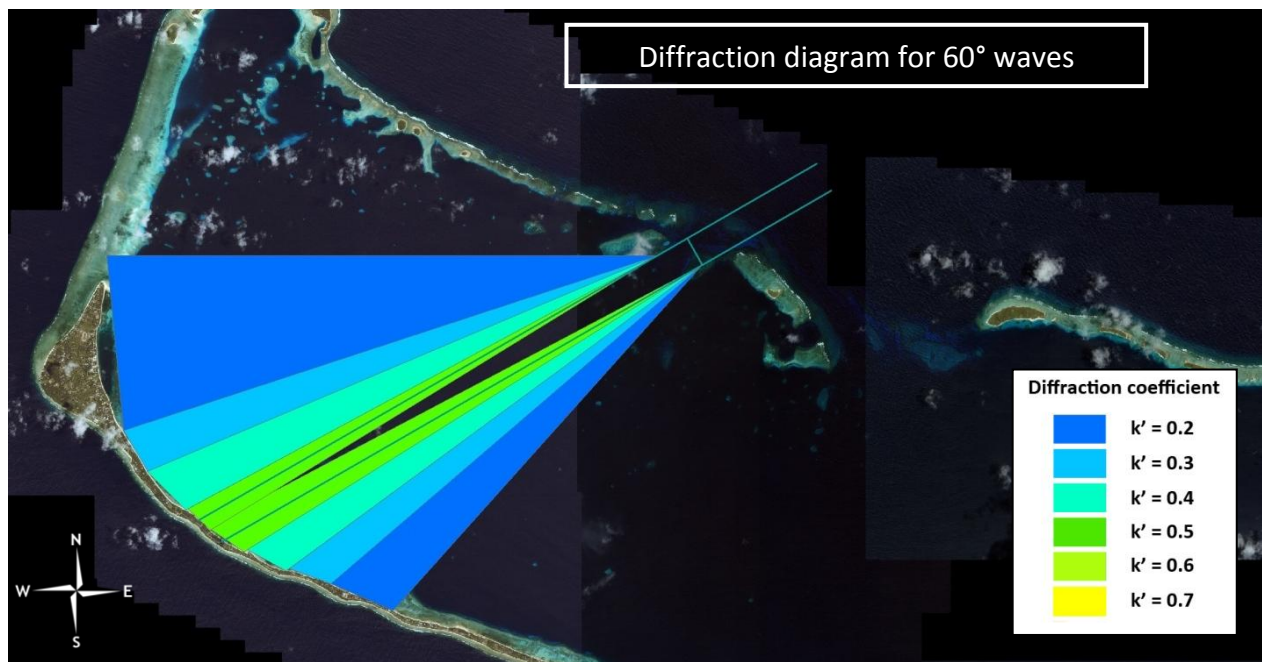


Figure 4.14 Diffraction diagram for correction coefficient k' for the small opening for 60° waves. (IKONOS 2001)

The shoreline was divided into 1000-m sections, each section having a specific tangent and normal (Figure 4.15). The angle between the wave direction and the normal was determined and employed to calculate the longshore sediment transport (Q), with the calculated wave height and angle between the normal and the incoming wave direction as input to the calculations. The calculations were made for both 22.5° and 60° wave angle approach. Full tabular values are given in Appendix VII.

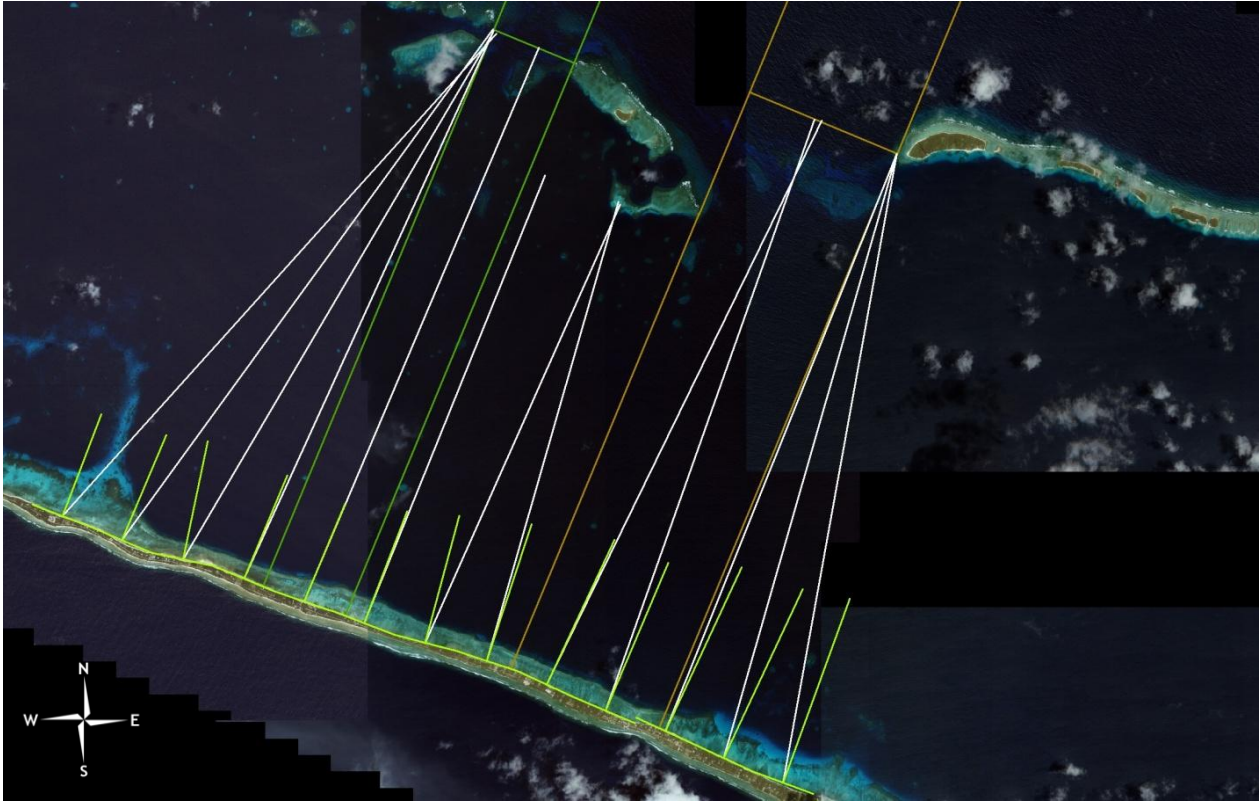


Figure 4.15 Shoreline sections of 1000 m with normal and diffraction angle. (IKONOS 2001)

4.4 Longshore sediment transport (LST)

The total longshore sediment transport rate is a measurement of the parallel movement of beach sediments along a beach section within the surf zone caused by breaking waves and surf (U.S. Army Corps of Engineers, 2002). It is an essential component to consider in coastal engineering management when investigating changing coastal areas regarding erosion or accretion.

Waves breaking at an angle to the coast, generating longshore currents and mobilizing sediment, are the major contributors to the transport of sand along the coast. This transport can greatly vary from little to no transport at all to several hundreds of thousands of cubic meters of sand per year (U.S. Army Corps of Engineers, 2002).

4.4.1 Longshore sediment transport processes

Winds and waves are related and change constantly, which may cause the sediment transport direction to change on a seasonal or diurnal basis. To determine the direction of the sediment transport is almost equally as important as estimating the quantity of the transport for studying coastal erosion and designing and managing coastal structures. Positive and negative directions are assigned to the transport in order to be able to determine and estimate the net and gross annual transport (U.S. Army Corps of Engineers, 2002).

4.4.2 Direction and magnitude of longshore sediment transport

The net direction of the longshore sediment transport is derived from the long-term sum (usually a decade or more) of many individual transport values. Indicators of transport direction can be found from major structures acting as sediment barriers, shoreline displacements, growth of longshore sand pits, and other depositional features. Grain size and composition of sediments can also be used as an indicator of transport direction as the grain size may decrease alongshore. However, there are other factors such as variation in wave energy which may cause changes in grain size. This method should be used with caution (U.S. Army Corps of Engineers, 2002).

4.5 Predicting potential longshore sediment transport on Majuro

The most commonly used formula for longshore sediment transport is the CERC formula developed by the US Army Corps of Engineers. However, the formula used for predicting potential longshore sediment transport in this report was proposed by Bayram, Larson, and Hanson (2007). The new formula is based on a number of high-quality data set from the field and laboratory environment, mainly collected at the U.S. Army Corps of Engineering Field Research Facility and the Coastal and Hydraulics Laboratory of the US Army Engineering Research and Development Center (Bayram, Larson, & Hanson, 2007). The new formula includes sediment transport generated by wind and tidal-currents, which most existing formulas on longshore sediment transport does not, and it is also sensitive to the sediment properties. The longshore sediment transport rate is given by,

$$Q_{lst} = \frac{\varepsilon}{(\rho_s - \rho)(1 - a)g w_s} F \bar{V} \quad (4-3)$$

where Q_{lst} is the longshore sediment transport rate in volume per unit time. It is important to understand that the formula only gives the total longshore sediment transport over a cross section on the beach assuming unlimited supply of sediment. A complete description of the formula is given in 0.

The main input quantities for the longshore sediment transport are wave direction, wave energy, and shoreline orientation. Since the majority of the winds are coming from a sector north to east (0) the most affected parts are located on the south and west side of the island.

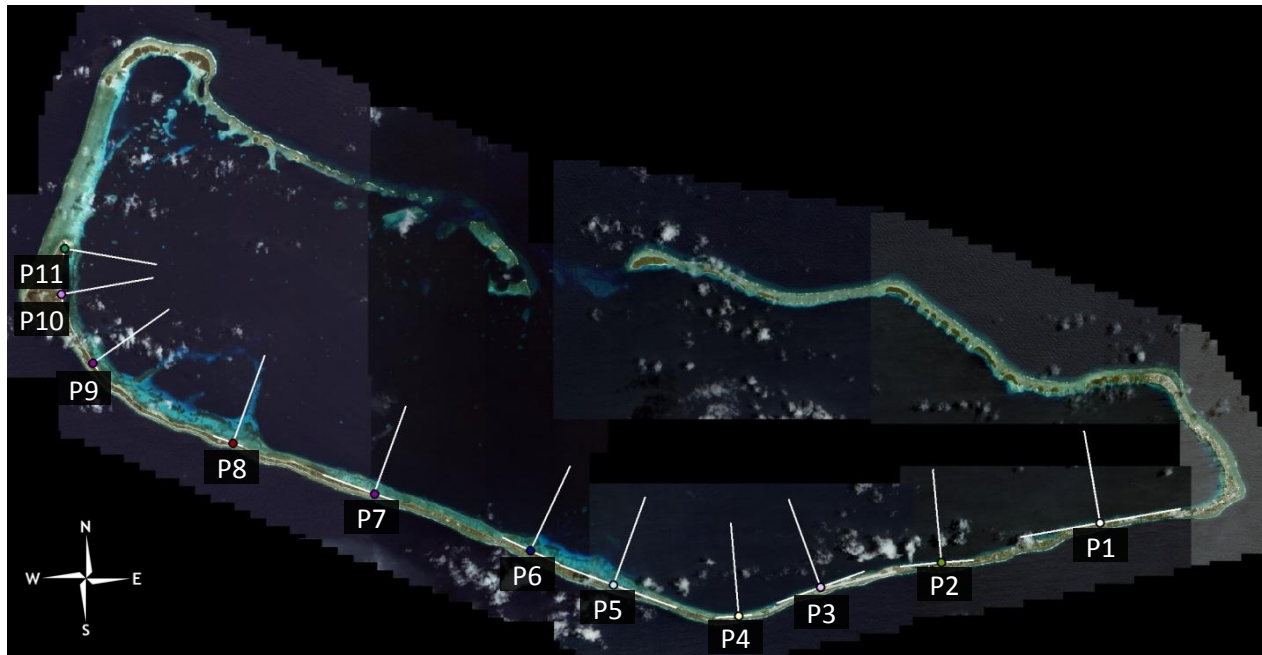


Figure 4.16 Locations for of sediment transport calculations and directions of the normal. (IKONOS 2001)

Eleven locations for calculations were selected along that lagoon shoreline (Figure 4.16), each location being associated with a normal and a fetch length for every 22.5° angles in the lagoon (Figure 4.17). The locations were chosen to represent shoreline stretches with approximately constant orientation. Each calculated wave from the wave climate in the lagoon from 1968 to 1999 was assigned a fetch length depending of the wave direction. The wave direction also made it possible to identify the incoming wave angle in comparison to the normal for each location. Combining all fetch lengths with all incoming wave angles and sediment and water properties in the formula by Bayram, Larson and Hanson (2007), the sediment transport was calculated for each wave at each location.

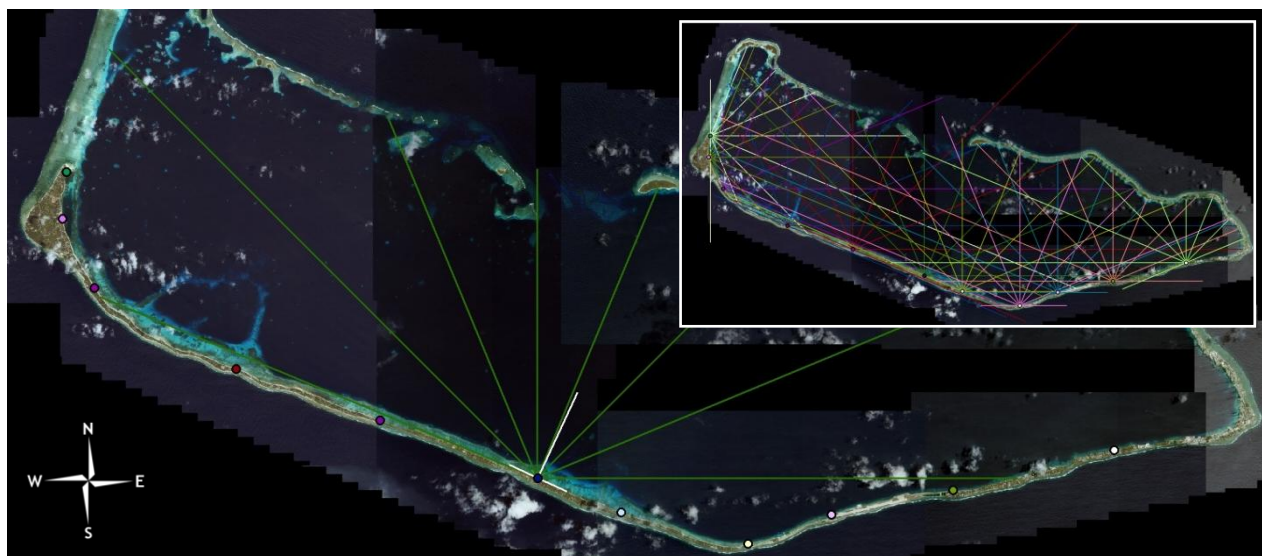


Figure 4.17 Example of fetch lengths for a location in the lagoon and an insert showing all fetch lengths. (IKONOS 2001)

4.6 Wave runup and dune/berm impact

Wave runup is the vertical height between the still-water level to the maximum height which the wave reaches up on the beach. The runup depends on the shape and roughness of the beach (i.e., sediment properties), water depth, bottom slope, and the characteristics of the incoming waves (U.S. Army Corps of Engineers, 2002). The wave runup phenomenon has been the subject of several studies, but due to large numbers of variables a considerable amount of uncertainty still remains in predicting it.

Beach profiles are in constant change. In conditions of waves attacking high up on the beach during a certain period of time the beach will erode and sediment will settle further down on the beach creating a protective bar on the beach slope (Figure 4.18). In times of smaller waves most of the sediment will return to the upper part of the beach.



Figure 4.18 Example of eroded beach and beach berm on Majuro. (H. Rapp)

4.6.1 Wave runup on Majuro

Buildup of large waves in the Majuro lagoon is rare, but due to the large variation in tidal elevation and the low topography even small waves may reach the beach berm, when high tide and large waves co-exists. If there is sufficient energy in the incoming waves at high tide that is dissipated across the profile there is risk of erosion.

Statistical data on the local wind speed and direction were employed to generate a wave climate in the Majuro Lagoon. Using this wave climate combined with the sea level change (mostly due to the tide), the runup was calculated using the Hunt formula (the beach slope was estimated to be about 8 % at the berm):

$$\frac{R}{H_0} = \frac{\tan\beta}{\sqrt{\frac{H_0}{L_0}}}$$

(4-4)

Hunt's formula is mostly used when designing structures and is usually considered to produce overestimations. One aspect that Hunt does not take into account is the incoming angle of the waves. The wave height was therefore been adjusted according to:

$$H_0' = H_0 \cdot \sqrt{\cos\alpha_0}$$

(4-5)

Previous studies have been carried out regarding beach profile change on Majuro. However, these field works are mostly limited to the coastal areas on Laura and to the city center of Majuro. In the city center most of the coastline is covered by hard structures as urban areas has grown in recent times.

Beach profiles were recorded along nine different lines by SOPAC on Laura in 1997 and 1998 (Figure 4.19). The profile evolution along these lines was later followed up by Ibaraki University, Japan, through field measurements led by Professor Hiromune Yokoki. Profile 8 is the most suitable lagoon-side profile and was chosen for runup calculations. Profiles 3 and 4 are on the ocean side, 5 to 7 are too close to the lagoon opening on the western side of the island (negligible wave energy is entering into the lagoon here), which may affect the results because of tidal currents, and profiles 1, 2 and 9 were not studied in the Japanese field campaign.

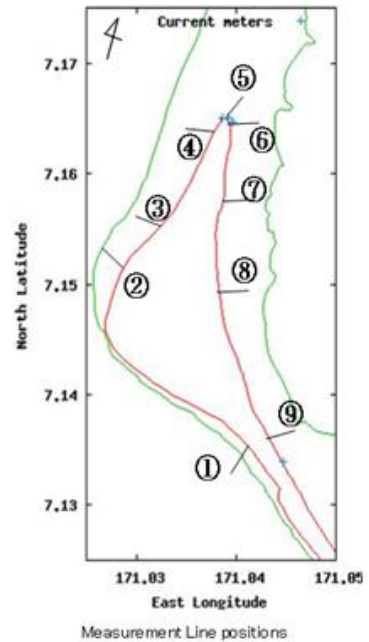


Figure 4.19 Location of beach profiles measured by SOPAC. (Yokoki 2009)

A comparison for Profile 8 was done between the earliest profile measured in February 1997 by SOPAC and the latest one measured in August 2009 by Professor Yokoki (Figure 4.20). The profile will probably differ somewhat during the year because of seasonal changes, which in this comparison might be the case as the first field study was done early in the year and the other about 6 months into the year. However, in the present analysis we are only interested in the change on the upper part of the beach to observe how much and at what rate the beach is retreating inland, and these changes are not related to seasonal variations on Majuro.

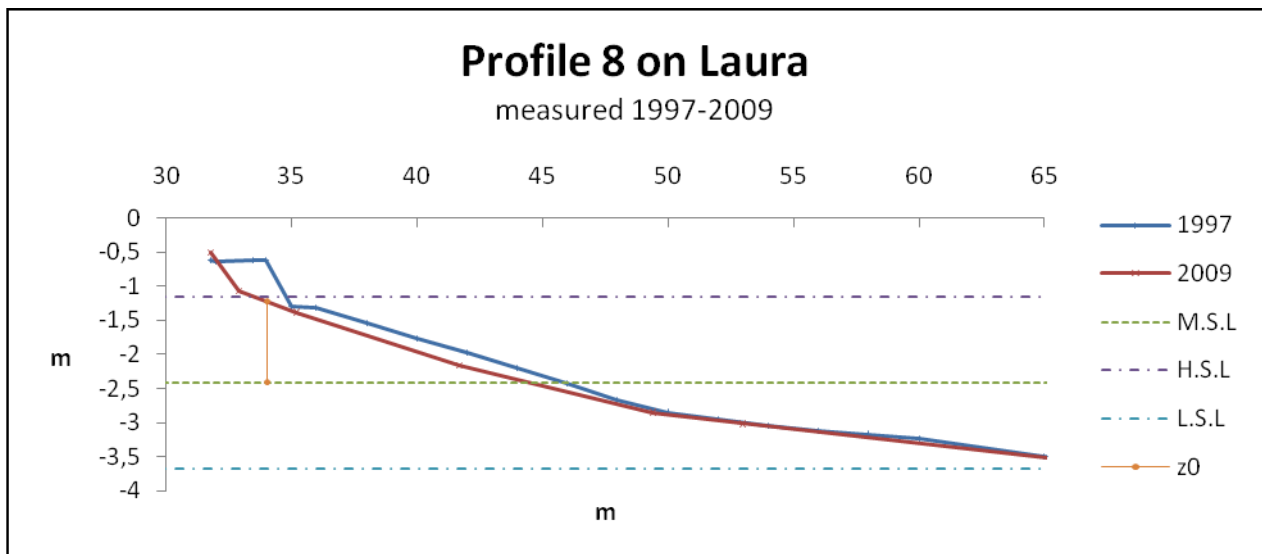


Figure 4.20 Beach profile 8 on Laura measured by SOPAC and Yokoki. (Woodward & Woodward, 1998 & Yokoki 2009)

4.6.2 Dune and berm erosion on Majuro

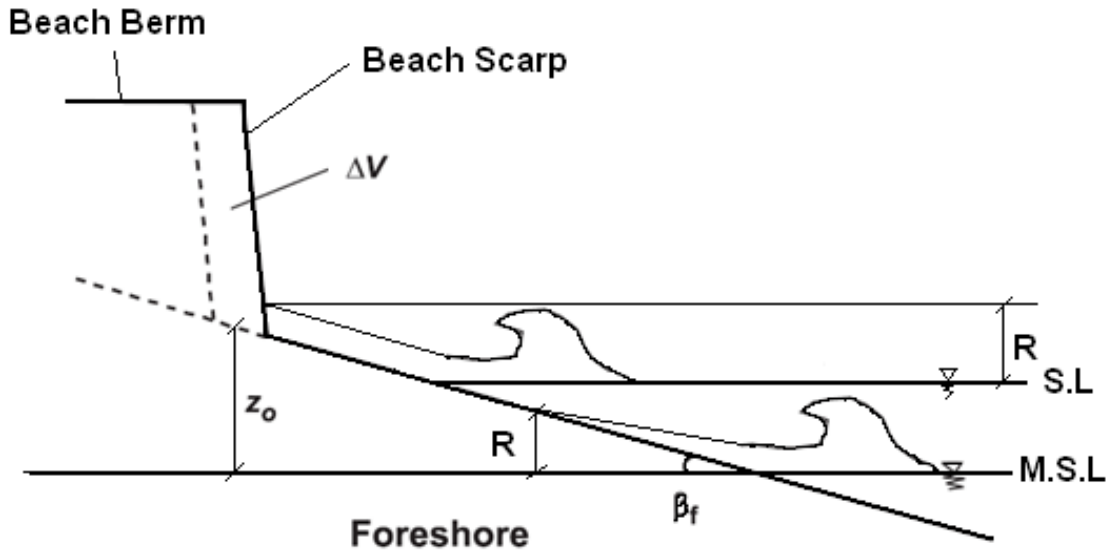


Figure 4.21 Schematic description of berm erosion due to wave impact in the presence of a scarp. (H. Hanson tvrl.lth.se)

For calculating berm erosion, the results from the wave runup must be combined with the slower variation in the water level associated primarily with the tide. By using the calculated wave climate in the lagoon during the period from February 1997 to August 2009 and combining it with the concurrent sea level data, estimations can be done of how often and what impact the waves may have on the berm. For erosion to occur, the current sea level and the runup must be greater than the berm foot elevation z_0 (Figure 4.21).

To estimate the erosion caused by wave impact, the dune erosion model developed by Larson et al. (2004) was employed. This model contains an empirical erosion coefficient C_s that relates the force exerted by the waves impacting the scarp and the weight of the volume of sediment eroded. The wave impact erosion model is written:

$$\frac{dV}{dt} = (-) 4 \cdot C_s \frac{(R - z_0)^2}{T} \quad (4-6)$$

where $\frac{dV}{dt}$ is the eroded volume per unit time (negative), R is the runup height with respect to the still-water level, z_0 the vertical distance from the current water level to the berm foot, and T is the wave period.

The beach berm was eroded from 1997-2009 in Profile 8 (Figure 4.20) corresponding to a volume of approximately of $1 \text{ m}^3/\text{m}$ (2 m of shoreline). For $1 \text{ m}^3/\text{m}$ of erosion, using a representative wave climate, C_s was calibrated to $3 \cdot 10^{-5}$. In this calculation 107 085 hours of wind data from 1997-2009 was used from the Majuro SEAFRAME Station to simulate waves reaching the shoreline at Profile 8. Only about 0.5 % of

the total waves reaches over z_0 and erodes the berm. For each individual wave in the time series that reaches the berm, a C_s -value may be obtained from:

$$C_s = \frac{dV}{4 * \frac{(R - z_0)^2}{T} dt} \quad (4-7)$$

The contribution from each wave in the time series combined with the total eroded volume will yield an overall C_s representative for the entire period. The C_s -values calculated in laboratory tests is normally in the range of 10^{-3} to 10^{-4} for sand dunes, although it is typically significantly smaller for field conditions. In this case the calculated C_s -value for Profile 8 is lower, and the reasons could be many, including the presence of vegetation for example. Vegetation could be a significant factor as it contributes to binding the sediments and preventing erosion. Should C_s been changed to a value of $5 \cdot 10^{-4}$, with the current conditions for Profile 8, the berm would erode about 15 times as fast, resulting in a berm retreat of 20-30 m. It is likely that z_0 will change over the years as the beach will adjust to a natural state; however, in the present calculations a mean value of z_0 has been chosen.

4.7 Ocean-side overtopping on Majuro (DUD)

Overtopping is when waves wash over natural or manmade barriers along the shoreline. There have been occasions when overtopping has been observed in the eastern parts of Majuro. The most recent event was recorded on the 9th of December 2008 (Figure 4.22) and is believed to have coincided with high waves generated by a low-pressure weather system in the Wake Islands, 500 miles north of Majuro. Although the high-tide at the time was only about 1.63 m compared to the mean sea level of 1.04 m, the consequences were severe. The fact that overtopping occurred under these circumstances raises questions concerning the consequences of future sea-level rise and climate change.

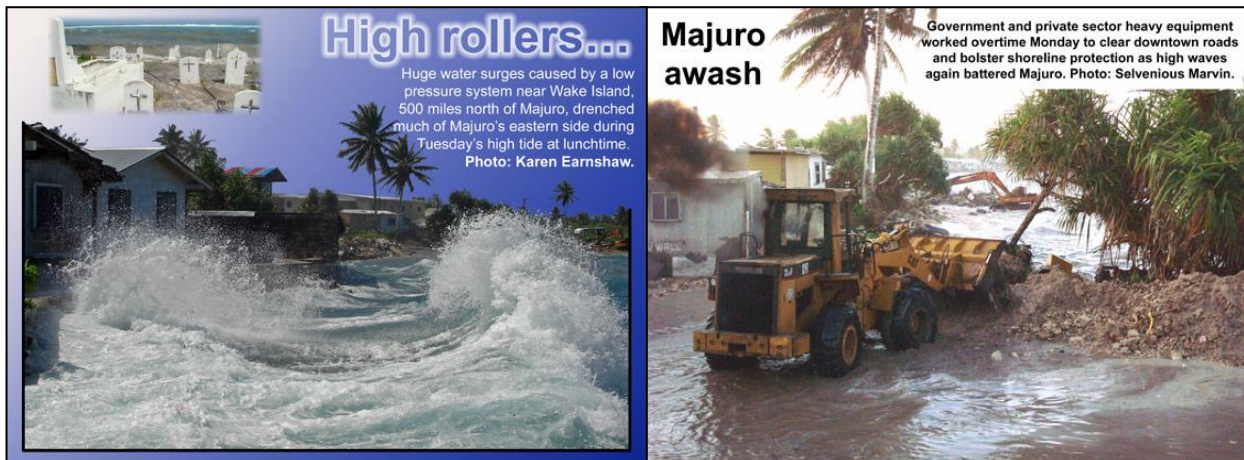


Figure 4.22 Overtopping on Majuro (Marshall Island Journal, December 2008)

It is not uncommon that the tide reaches over 2 m, and on these occasions the water hardly reaches the shore. However, although the tide itself does not reach very far upon the reef-flat, the combination of high tide and large waves may create high water levels because of wave set-up on the reef.

4.7.1 Wave set-down and set-up

Seaward of the break point a set-down is created due to changes in the momentum flux of the waves, implying that the mean water level is lower than the still water level. Shoreward of the break point a wave set-up is created instead. Here, the waves lose momentum through the breaking process, which is compensated by a pressure gradient generated by the upward slope of the water surface (Figure 4.23) (U.S. Army Corps of Engineers, 2002). The mean water level induced by the wave set-up intersects the beach at a location above the still-water level.

The city center DUD, located on the east part of Majuro, is exposed to the largest swells from the ocean. The wave set-up causes a buildup of water on the reef flats on Majuro, allowing waves that normally should break on the reef edge to travel on top of the reef and break on the shore. This phenomenon may cause overtopping in rare cases.

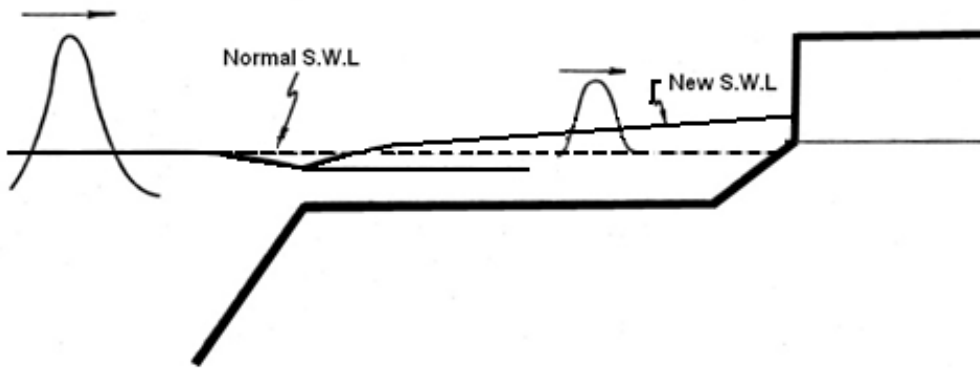


Figure 4.23 Example of wave set-down and wave set-up. (U.S. Army Corps of Engineers, 2002)

The risk of overtopping on Majuro was evaluated from at chosen location on DUD (Figure 4.24) using wave data from KMNI that included tabulated significant wave height (Appendix IX) between 1971 and 2001. According to KMNI, 18% of the total waves have a direction 0° - 45° and 0.6 % of the waves are between 4 and 5m. Furthermore, 38 % of the total waves have a direction 45° - 90° and 0.3 % of these waves are between 4 and 5m. Of the total waves, only 0.2 % is between 4 and 5 m and comes from a critical direction.

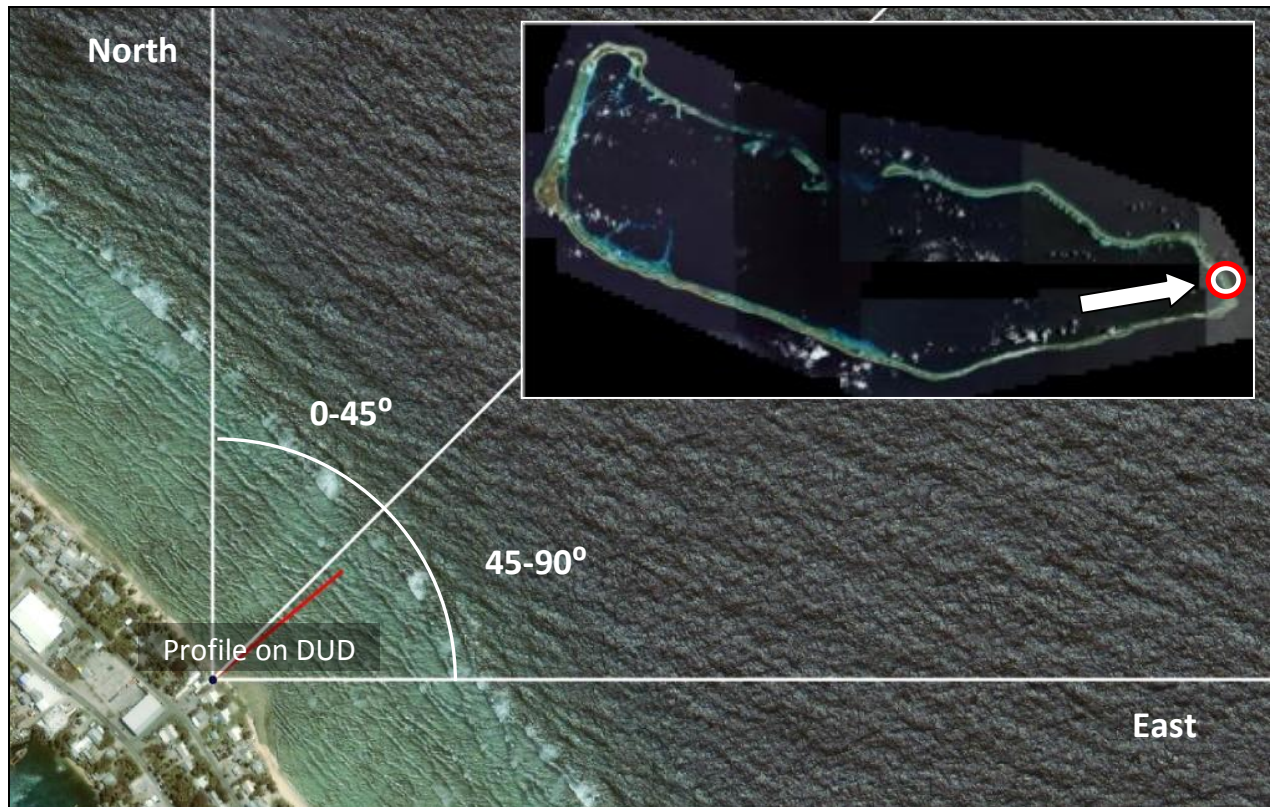


Figure 4.24 Chosen location for evaluating overtopping on Majuro. (IKONOS 2001)

Using the formula presented by Dalrymple (1984) estimations of the wave set-up from the large swell waves can be calculated.

$$n = \frac{\frac{3 \cdot k^2}{8}}{1 + \frac{3 \cdot k^2}{8}} \cdot h_b$$

(4-8)

The wave set-up due to breaking is denoted n , the depth at incipient breaking is h_b , and k is the breaker depth index. The significant wave height is used to estimate the wave set-up, which may in some cases generate a lower breaking wave height than some of the individual waves making up the random wave field. However, as a representative wave that produces sustained overtopping this measure was judged to be satisfactory. The maximum wave height of 5 m and a breaker index of 0.78, results in a wave setup of 0.93 m, when adding the wave, which can be estimated as 0.78·0.93, the result of the total water height close to the seawall becomes 1.65 m (distance A in figure 4.25) which is close to the distance between the still water level and the top of the seawall in the case when overtopping occurred in 2008 (Figure 4.25) using the recorded tidal elevation. A wave height of 4 m yields a mean water surface displacement of 1.32 m (distance B in figure 4.25), which is close to the distance between the sea water level and the top of the seawall when the tide is close to 2 m (Figure 4.25).

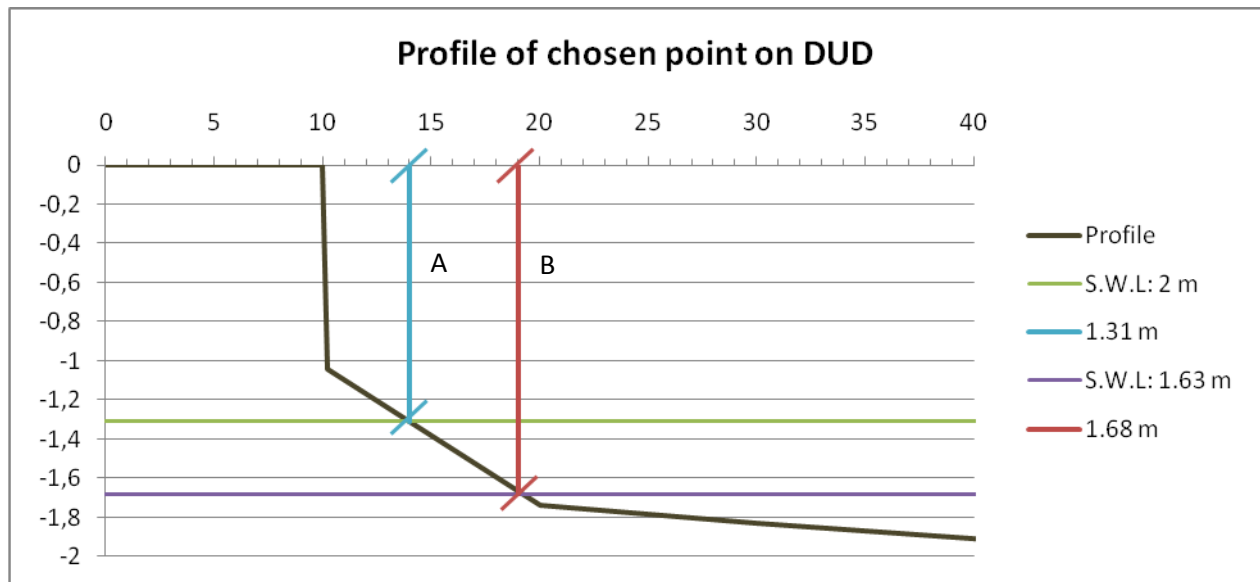


Figure 4.25 Profile of the chosen point on DUD for overtopping evaluation.

To calculate the total sea level on the ocean side, tidal data must be combined with wave height data. Although tidal variations on Majuro are available on AusBOM (2010), the wave data from KMNI is presented as joint probability distributions for wave height, period, and angle. Thus, it is not possible to analyze wave properties and water levels jointly. In order to assess the risk of overtopping the tide and the waves have to be regarded as belonging to two different independent probability distributions. The resulting probability of two events occurring is estimated by multiplying their individual probability of occurrence.

5 Future sea-level rise scenarios

The IPCC Special Report Emission Scenarios (SRES) were first introduced in 1990 and have since then been continuously evaluated and updated. The several climate change models developed by IPCC are based on the complex relationship of observed statistical climate data and the driving forces of climate change such as emissions of greenhouse gases (Nakicenovic, et al., 2000).

IPCC presents in their Fourth Assessment Report (AR4) 2007, six different future scenarios. In the AR4, IPCC claims that by 2090-2099, the temperature will rise between 1.1 and 6.4 C° and the global sea level will rise 0.18-0.59 m. In 2008, The Delta Committee released an updated future scenario with a sea-level rise between 0.25 and 0.76 m based on IPCC's 2007 report, including extra discharge from melting icecaps (Delta Committee, 2008). The sea-level rise trend from SEAFRAME at Majuro and the sea-level rise scenario from the Delta Committee will be used in this report.

Due to the uncertainty and extreme acceleration in sea-level rise predicted between 2100 and 2200, the chosen scenarios will not go past 2100, although the estimated sea-level rise value of 3.5m by 2200 (Delta Committee, 2008) will be used to approximate how the acceleration in sea-level rise occurs until 2100.

5.1 Chosen sea-level rise scenarios

Table 5.1 Chosen future sea-level rise scenarios by 2100 on Majuro

Scenario 1	Scenario 2	Scenario 3
Delta Committee 0.25 m sea-level rise by 2100	SEAFRAME 0.44 m sea-level rise by 2100	Delta Committee 0.76 m sea-level rise by 2100

Table 5.1 summarizes the future sea-level rise scenarios assumed in this study. Although IPCC indicates the possibility of increased wind speeds and change in wind direction in the future as reported by Mimura, et al. (2007), there is no quantitative information on the kind of change that might occur. For that reason, future changes in wind speed and wind direction are not included when regarding various sea-level rise scenarios.

5.1.1 Scenario 1

In Scenario 1, the lower range of 0.25 m sea-level rise by 2100 from the Delta Committee 2008 scenario is assumed. In this case a linear increase in sea level is adopted, resulting in a sea-level rise of 2.5 mm/year until 2100 (Figure 5.1).

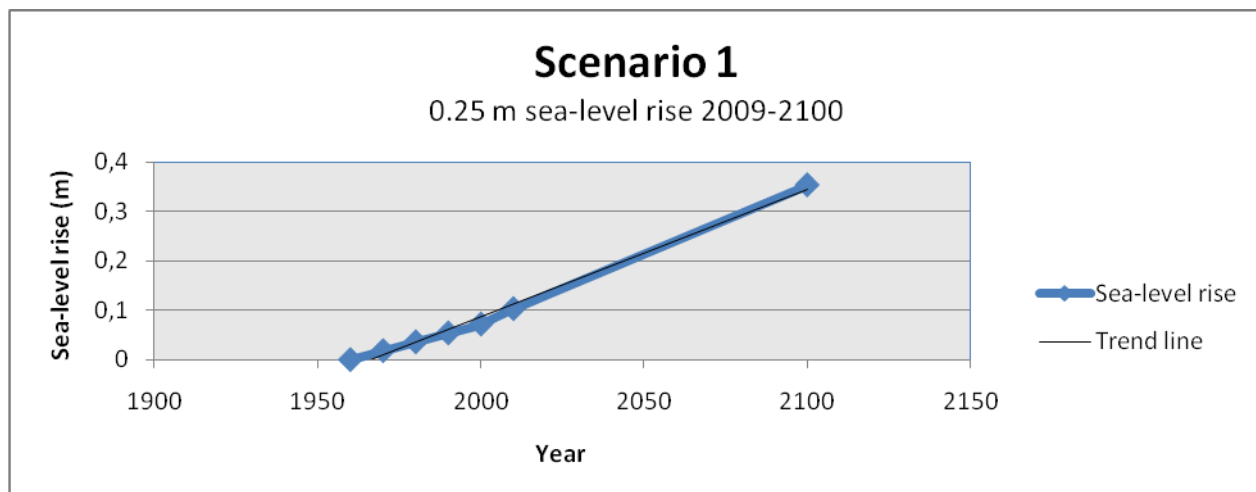


Figure 5.1 Sea-level rise for Scenario 1.

5.1.2 Scenario 2

The second scenario is solely based on the current sea level trend of 4.4mm/year at Majuro taken from observed data at the Majuro SEAFRAME station (Figure 5.2). The scenario spans over about 100 years to 2100.

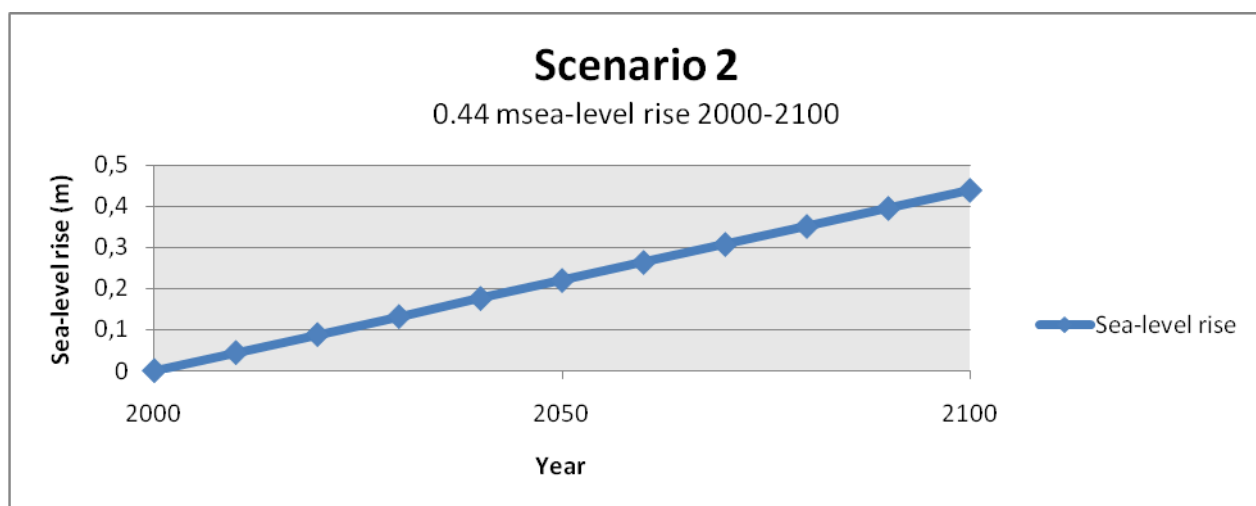


Figure 5.2 Sea-level rise for Scenario 2.

5.1.3 Scenario 3

Scenario 3 assumes the upper range sea-level rise of 0.76 m by 2100 from the Delta Committee. The highest sea-level rise scenario by both IPCC and the Delta Committee shows an accelerating sea-level rise with time (Figure 5.3). By using a local upper limit scenario for year 2200 given in the Delta Committee, 2008, an equation was fitted to the plotted values. An adjusted sea-level rise for 2009-2100 based on the plotted trend line was then added and the sea-level rise was calculated every ten years to simulate an accelerated sea-level rise in the future (Figure 5.4). The trend line was given by,

$$y = 2 \cdot 10^{-7}x^3 + 3 \cdot 10^{-5}x^2 + 0.002x. \quad (5-1)$$

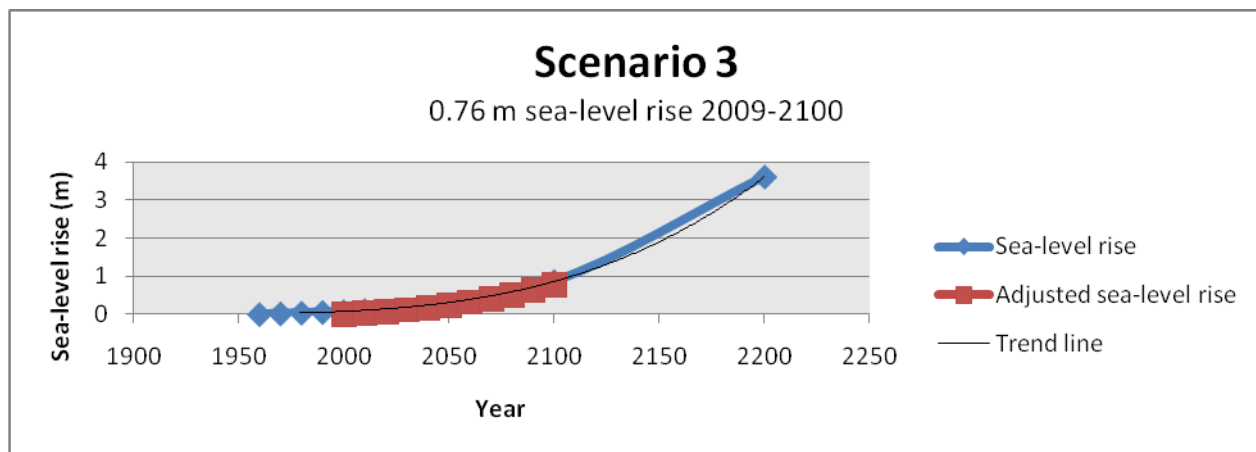


Figure 5.3 Sea-level rise for Scenario 3.

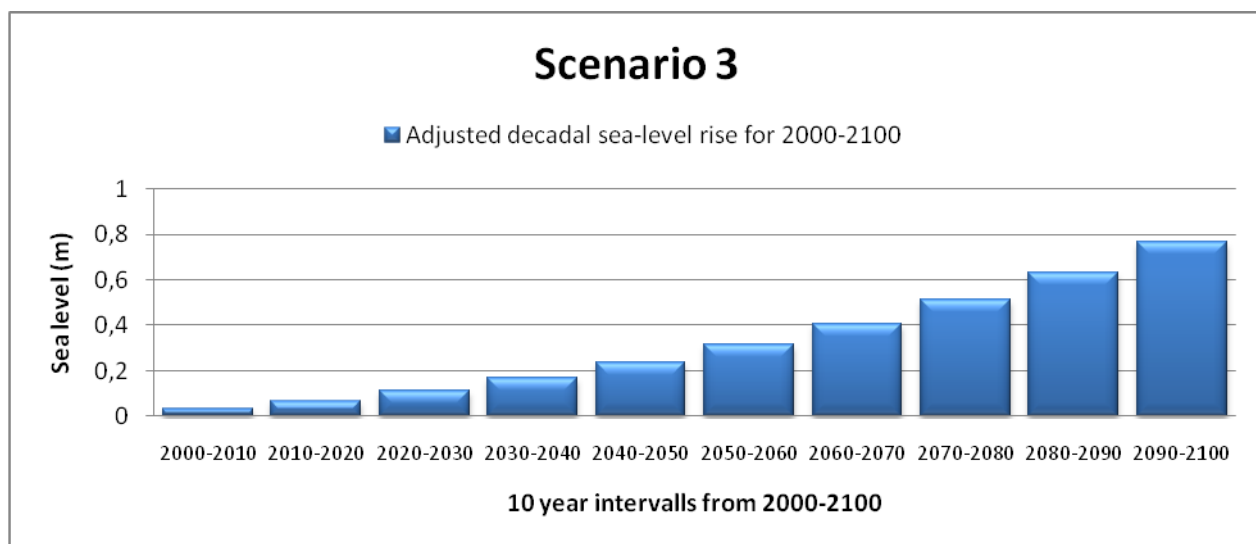


Figure 5.4 Average sea level every 10 years in Scenario 3.

5.2 Overtopping DUD

In scenarios of a possible sea-level rise, overtopping calculations are based on the percentage of time the water level is higher than 2 m using tidal data from 1971-2001 and the tabulated significant wave height. For some of these years there were missing values in the data, and in order to calculate over the whole time series the percentage of the sea-level reaching over 2 m for each year was established. A mean percentage for the whole time series was then employed. For all measured sea levels from 1971 to 2001, approximately 2 % of the sea levels reach over 2 m. Calculations of sea levels over 2 m for a sea-level rise of 0.2, 0.4 and 0.6 m was simulated by calculating the percentage of levels over 1.8 m, 1.6 m and 1.4 m. The result is presented in Table 5.2.

Table 5.2 Estimations of sea levels above 2m for different sea-level rise scenarios.

Sea-level rise	0 m	0.2 m	0.4 m	0.6 m
Sea levels above 2 m	2 %	7%	17%	30%
Waves over 4 m	0.2 %	0.2%	0.2%	0.2%

6 Results

6.1 Longshore sediment transport by diffraction

The yearly average sediment transport is calculated for each location using ocean side wave data from KMNI. The sediment transport for the two incoming wave cases at 22.5° were added and denoted **A** and the sediment transport for incoming waves at 60° were denoted **B**. The sediment transport magnitudes for the both cases are shown in Table 6.1 and Table 6.2 and the transport direction are displayed in Figure 6.1 and Figure 6.2.

Table 6.1 Sediment transport and direction for wave cases at 22.5° (Figure 6.1).

	A1	A2	A3	A4	A5	A6	A7
Q (m ³ /y)	-18593	-30598	-18412	-65733	18828	-23785	105233
	A8	A9	A10	A11	A12	A13	
Q (m ³ /y)	3653	19827	3804	27939	11463	7771	

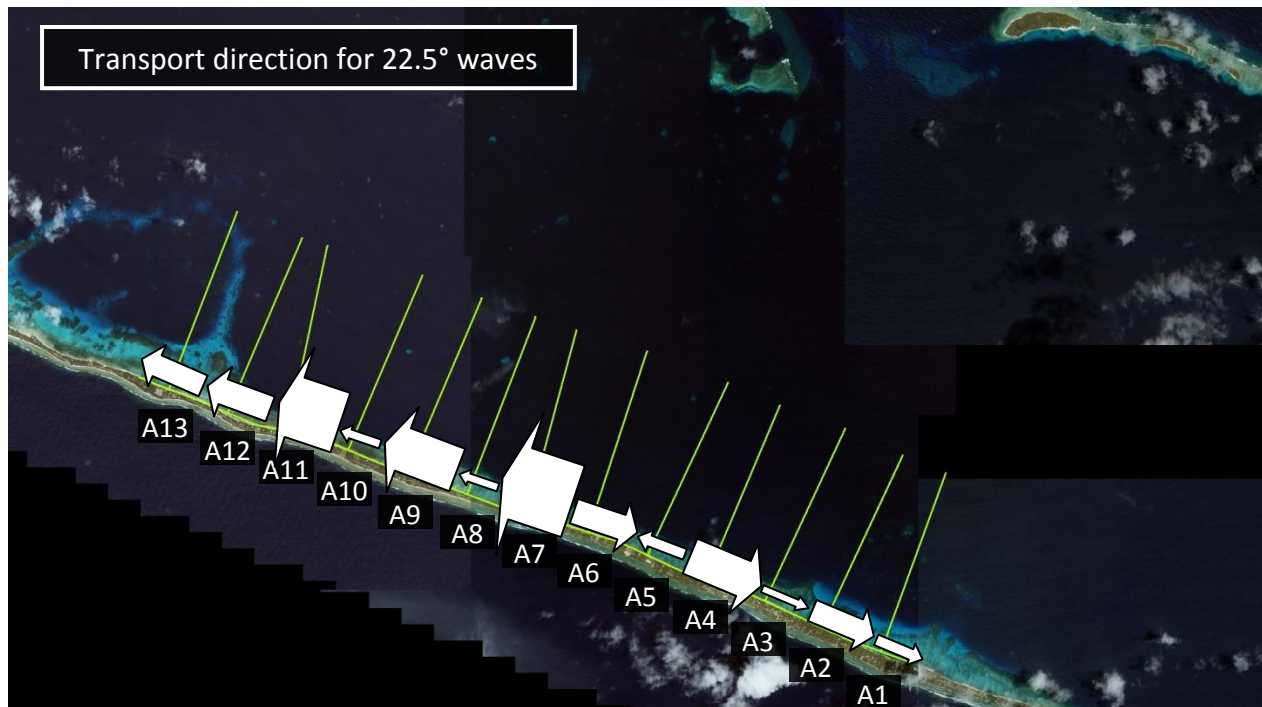


Figure 6.1 Sediment transport direction for incoming waves at 22.5°. (IKONOS 2001)

Table 6.2 Sediment transport and direction for wave cases at 60° (Figure 6.2).

	B1	B2	B3	B4	B5	B6	B7	B8	B9
Q (m ³ /y)	9445	32127	58838	82746	65483	27525	12665	5115	-1643

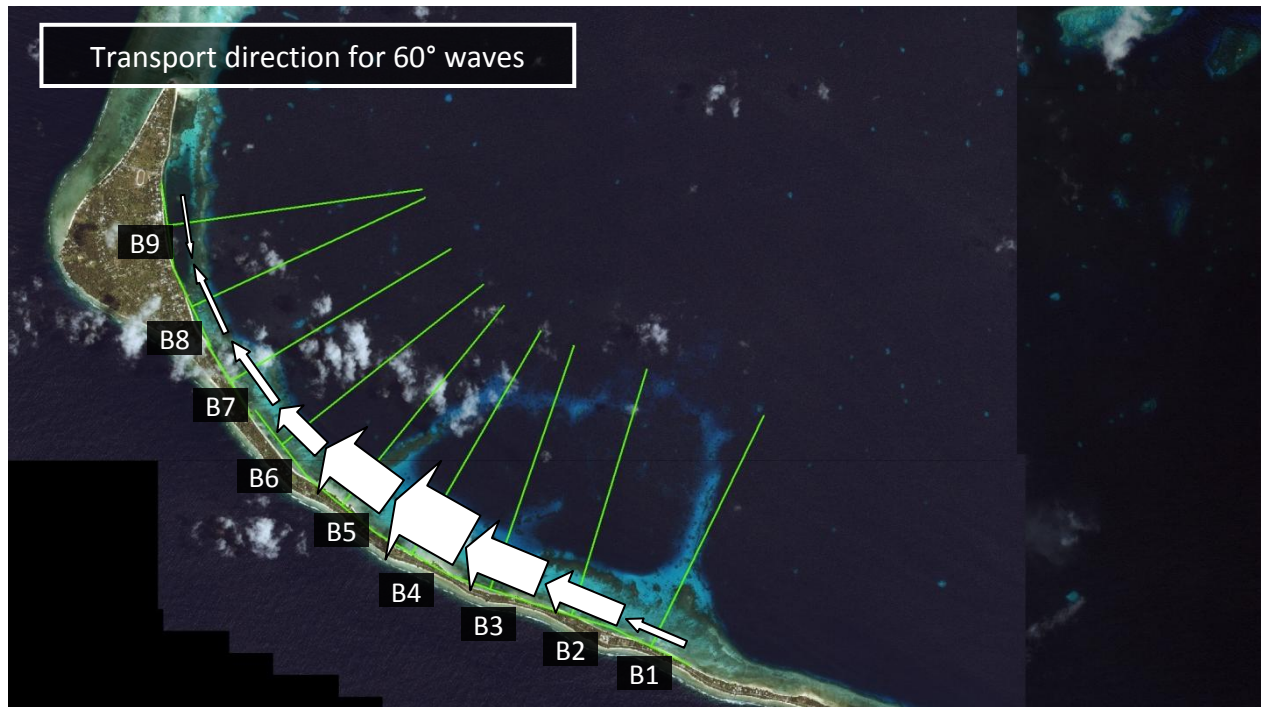


Figure 6.2 Sediment transport direction for incoming waves at 60°. (IKONOS 2001)

6.2 Longshore sediment transport by local waves

An average yearly sediment transport rate (Table 6.3) was calculated for each location using the SEAFRAME wind data at Majuro from 1994-2009 to estimate the generated waves and the formula by Bayram, Larson and Hanson (2007) to compute the total longshore sediment transport rate. The sediment transport direction is given in Figure 6.3, which confirms the sediment transport direction shown in Xue, 2001.

Table 6.3 Average yearly sediment transport at Majuro.

	P1	P2	P3	P4	P5	P6	P7	P8	P9	P10	P11
Q (m ³ /year)	6135	38805	26479	26796	29563	29116	36450	36480	12122	-5955	-7198

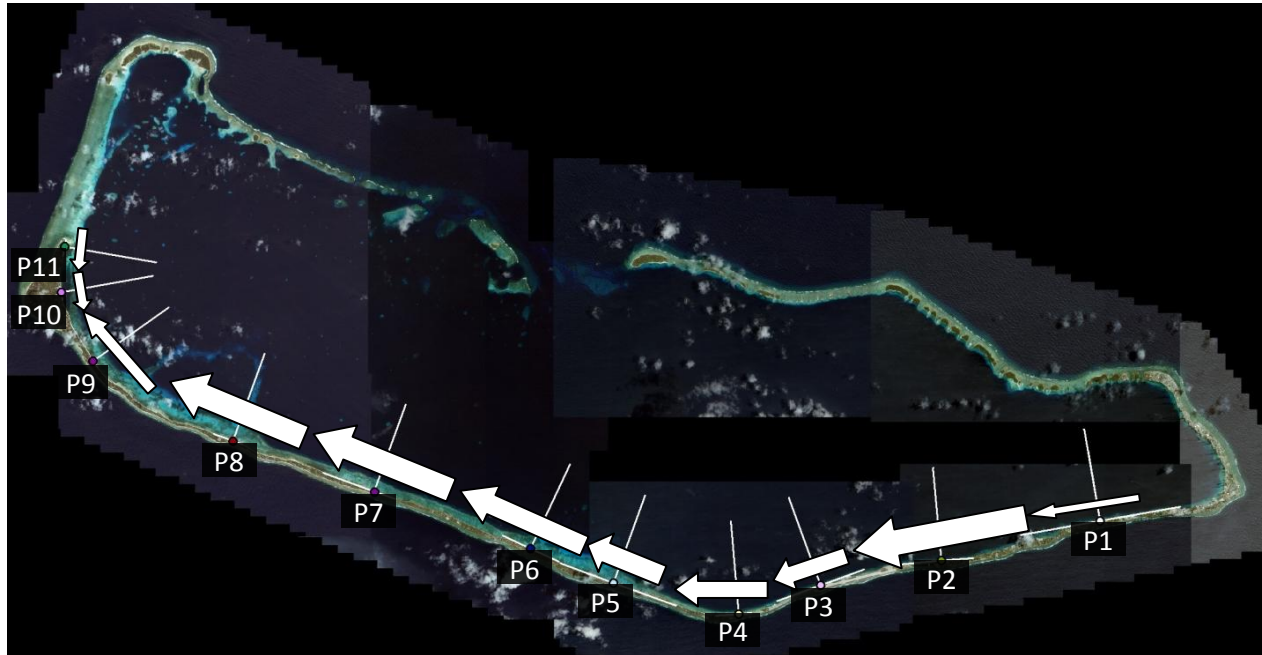


Figure 6.3 Sediment transport direction on Majuro Atoll. (IKONOS 2001)

A combination of sediment transport from both diffraction and local waves are presented in Table 6.4. The sediment transport from diffraction contributes to the total sum in extreme amounts at P7, P8, and P9. In the remaining points P5, P6, P9, and P10 diffraction contributes in the range of 50-60%. When combining the results from ocean waves and locally generated waves the transport changes direction at locations 2, 4, and 5. This partly contradicts the results presented by Xue (2001); his results were more in agreement with the longshore sediment transport caused by local waves only. Due to the lack of detailed information about the influence of diffracted ocean waves along this beach stretch and the simplifications done in the calculations, no firm conclusions can be made regarding the transport direction without additional data.

Table 6.4 Combining longshore sediment transport from diffraction and local waves

Diffraction	Q (m ³ /y)	Local waves	Q (m ³ /y)	Sum of Q (m ³ /y)
A1	-18593	P5	29563	-19628
A2	-30598			
A3	-18412	P6	29116	-36201
A4	-65733			
A5	18828			
A6	-23785	P7	36450	141378
A7	105233,5			
A8	3653			
A9	19827			
A10	3804	P8	36480	187867

A11	27939	P8		
A12	11463			
A13	7771			
B1	9445			
B2	32127			
B3	58838			
Diffraction	Q (m ³ /y)	Local waves	Q (m ³ /y)	Sum of Q (m ³ /y)
B4	82746	P9	12122	200541
B5	65483			
B6	27525			
B7	12665			
B8	5115	P10	-5955	-2483
B9	-1643			

6.2.1 Future sediment transport

The sediment transport formula shows that an increase in wind intensity will increase the sediment transport, since the wave height will increase. A 10% increase in wind intensity resulted in an almost 25% increase in sediment transport (Table 6.5). A future wind scenario has not been stated by IPCC. However, Mimura, et al. (2007) confirm a possible increase in the number of intense cyclones, although the total number may decrease on a global scale. It has also been indicated that a possible change in swell direction may occur and the potential impact such a change could have on small islands. Due to large uncertainties, future wind scenarios will not be included in the three scenarios discussed in this report.

Table 6.5 Average yearly sediment transport based on a 10% uniform increase in all winds speeds.

	P1	P2	P3	P4	P5	P6	P7	P8	P9	P10	P11
Q _{+10% intensity} (m ³ /year)	8040	51574	18951	35246	38949	38359	48140	48228	16211	-7734	-9815

6.3 Runup and dune/berm impact for future scenarios

The number of runup occurrences will increase as sea level rises in time due to the increasing exposure of the beach berm to waves. Lacking data of the topography on the shoreward side, the runup calculation will only go as far as the measured beach profile stretches inland, comparing the volume per unit width between the profile topography and the current berm foot (z_0). The area of potential erodible material in Profile 8 shown in Figure 6.4 is estimated to be 25 m³/m, which is approximately 32 m inland retreat. The time steps for the future runup scenarios are divided in 10 year periods, providing a rough estimation of the time it takes for the beach to erode.

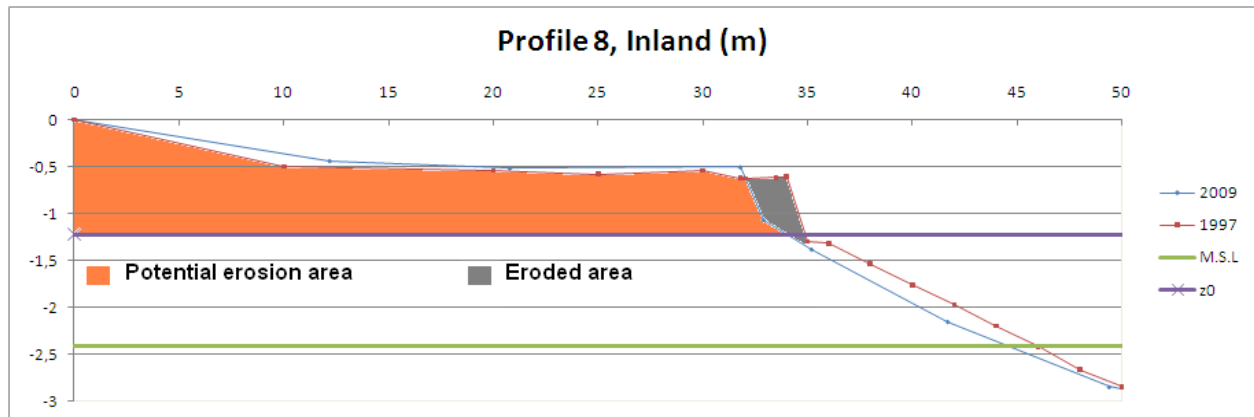


Figure 6.4 Potential erosion area for Profile 8.

6.3.1 No sea-level rise

If the water level remains constant, $0.73 \text{ m}^3/\text{m}$ of sand will erode every 10 years. If the erosion remains at this speed it will take approximately 300 - 400 years for the shoreline to move 32 m inland.

6.3.2 Sea-level rise scenarios

A summary of the future sea-level rise scenarios is given in Table 6.6 and the erosion for Profile 8 for every 10 years calculated for each sea-level rise scenario is shown in Figure 6.5, Figure 6.6 and Figure 6.7.

Table 6.6 Erosion in Profile 8 for 3 possible future sea-level rise scenarios

	Scenario 1	Scenario 2	Scenario 3
Rate	Delta Committee 0.25 m sea-level rise by 2100	SEAFRAME 0.44 m sea-level rise by 2100	Delta Committee 0.76 m sea-level rise by 2100
Type of increase	Linear	Linear	Exponential
Estimated time for 32 m retreat of Profile 8 from 2010	70-80 years	50-60 years	50-60 years

Despite that the calculations only goes as far as the measurements of beach profile 8 reaches inland, the results show a major increase in the 2nd half of the time period resulting in a loss of $50 \text{ m}^3/\text{m}$ with a sea-level rise of 0.25 m, $230 \text{ m}^3/\text{m}$ with a sea-level rise of 0.44 m, and $1100 \text{ m}^3/\text{m}$ with a sea-level rise of 0.76 m by 2100.

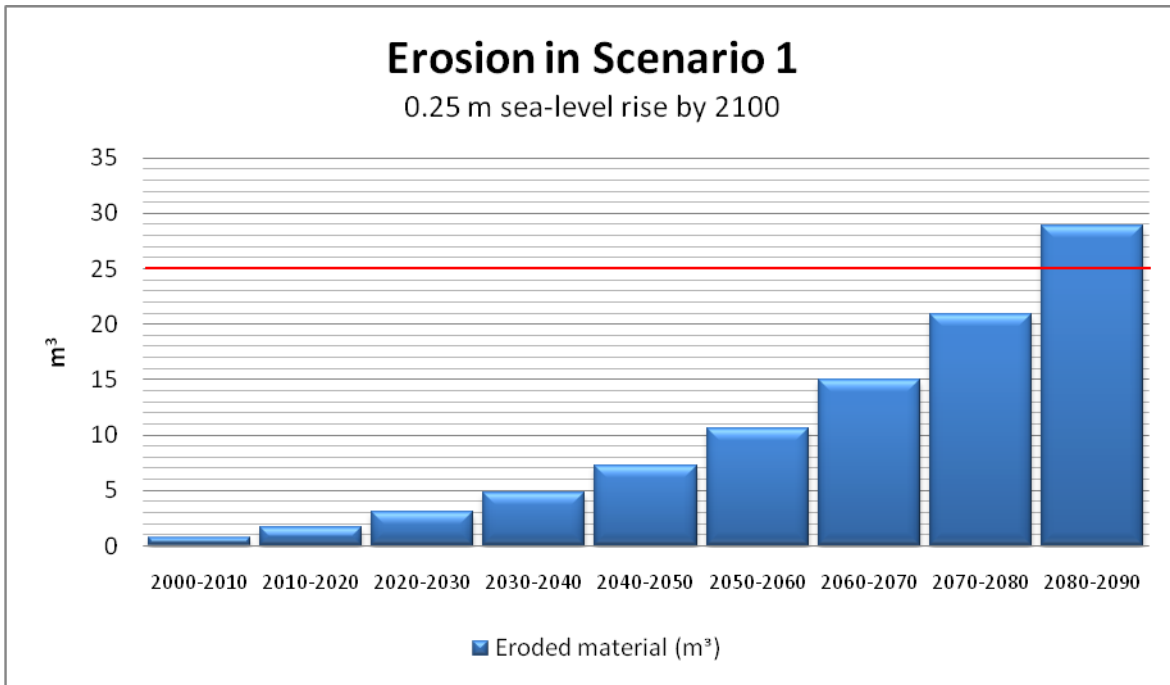


Figure 6.5 Erosion for Scenario 1 at Profile 8.

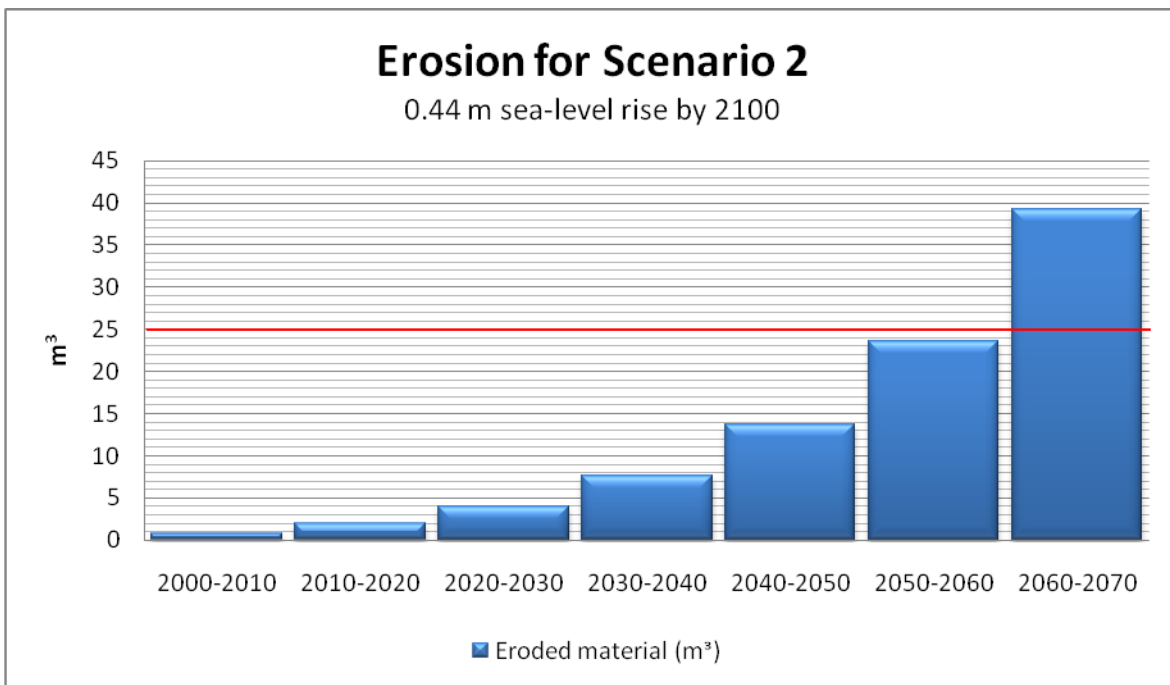


Figure 6.6 Erosion for Scenario 2 at Profile 8.

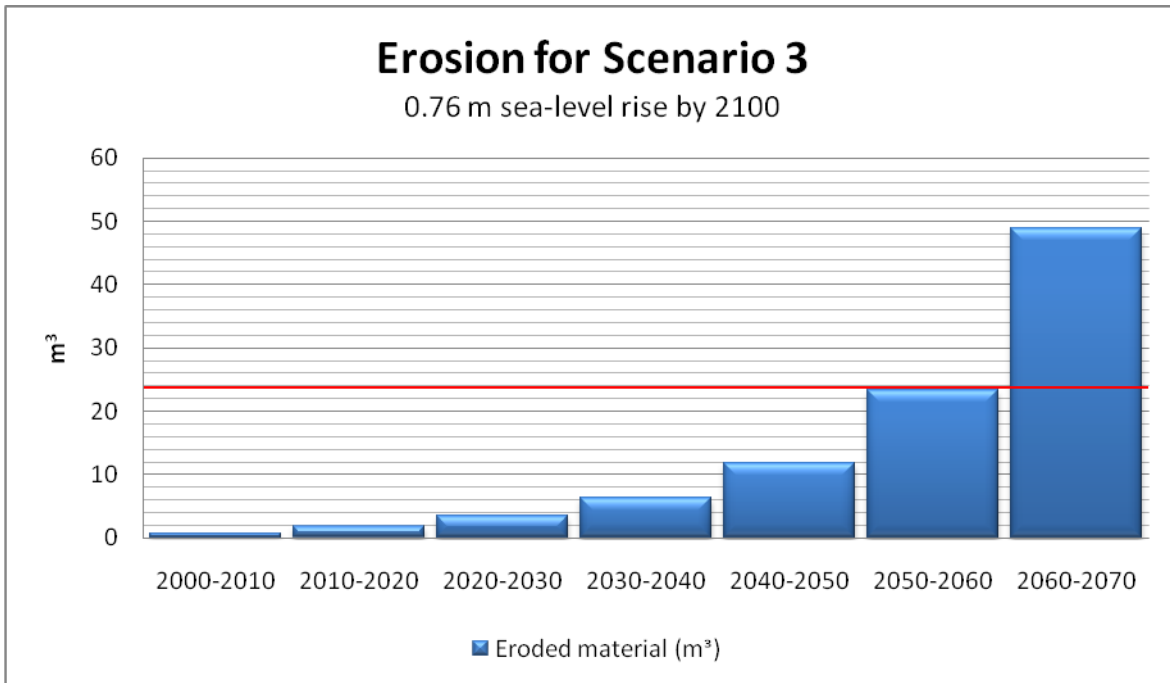


Figure 6.7 Erosion for Scenario 3 at Profile 8

Although the erosion follows a similar pattern in the beginning of the time period, the acceleration of the erosion has a very different magnitude during the latter half. Looking at the estimation in the years between 2050 and 2100 the speed of the erosion is exponential (Figure 6.8).

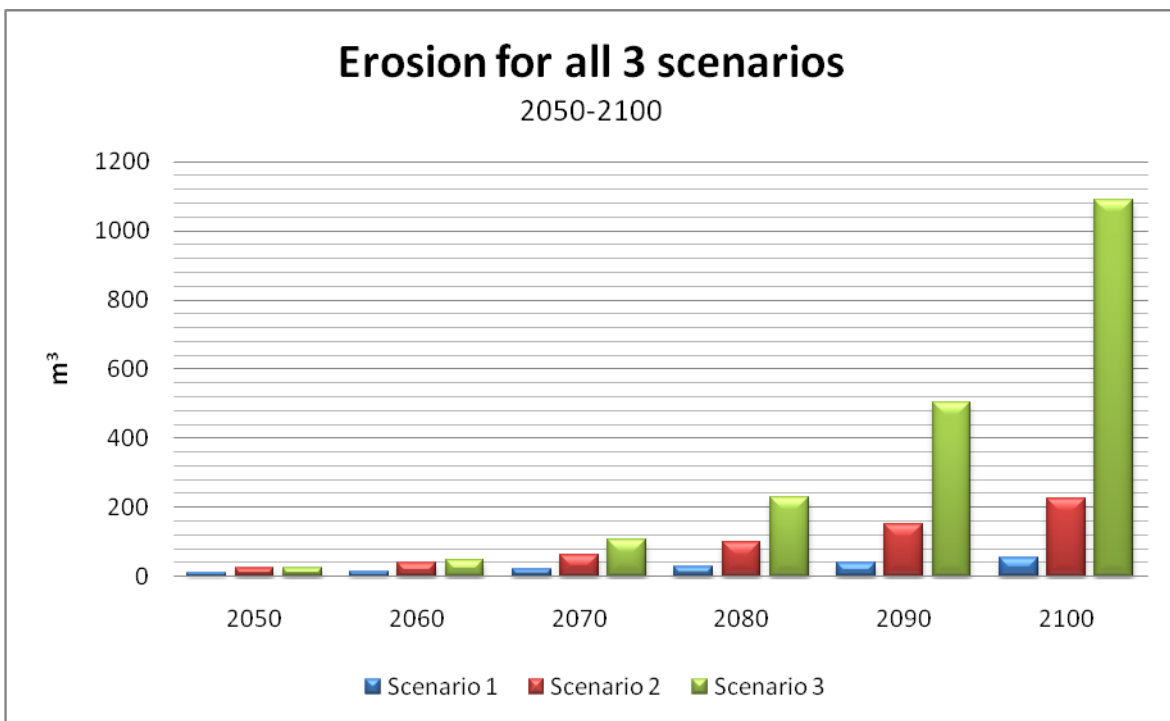


Figure 6.8 Erosion for all 3 scenarios at Profile 8 from 2050-2100.

6.4 Overtopping on DUD

The frequency of overtopping on Majuro is unknown, though at least one known occurrence has been recorded in 2008. Regarding at tide and extreme waves as independent events the exceedance probabilities can be multiplied with each other. Assuming that overtopping happens once at present conditions, the risk of overtopping on Majuro compared to existing tide and extreme wave conditions will become greater in the event of a sea level rise.

Table 6.7

Sea-level rise	0 m	0.2 m	0.4 m	0.6 m
Sea levels above 2 m	2%	7%	17%	30%
Waves over 4 m	0.2%	0.2%	0.2%	0.2%
Overtopping probability	1 time	3.5 times	8.5 times	15 times

7 Discussion

7.1 Longshore sediment transport on Majuro

Winds and waves are interlinked in a dynamic process, influenced by several other factors, for example temperature and barometric pressure. Wind speeds from the hourly wind data taken from Majuro SEAFRAME station in the presented calculations are assumed to be constant for the full hour. This however, could possibly be a source of error due to lack of information about whether the measured wind speed is an hourly average or one measurement per hour. The wave climate calculated for the lagoon may also include other sources of errors and may be regarded as rather simplified. Water depths in the lagoon were taken from a US Naval Sea Chart from 1944 and changes since then are likely to have occurred. The main uncertainty regarding the calculated wave climate is the coral reefs surrounding the atoll in combination with the tide. Coral does not grow above water under normal circumstances, providing an indication of a maximum coral height roughly around low tide. By comparing the water depth and breaking wave height ratio, all waves at high tide could be assumed to remain unaffected by the reef. However, coral environments are highly variable, thus making it difficult to predict its impact on incoming waves during tidal levels other than high tide.

Longshore sediment transport is even more so a complex and dynamic process with many factors contributing. The quantities calculated in the Results (Chapter 8.1) are based on unlimited sediment supply, which is typically not the case on Majuro Atoll. Sand and sediments are in fact a scarce resource, with exception on the western rim of the atoll at Laura. At many places, especially around the city centre at DUD, sandy beaches are completely absent and replaced with hard reef flats along with constructed sea walls protecting most of the urbanized coast lines. Large scale dredging projects on both lagoon and ocean side was initiated in the early 90's and have since then diminished vital portions of sand and sediments, causing a sediment deficiency in many areas. Over the last decade as sea walls and dredging became more common, it is likely that the human impact on coastal areas on Majuro have interrupted and disturbed the natural movement of the sediments.

The sediment transport induced from the ocean waves coming in through the northern openings are seemingly of great importance as it yields a longshore sediment transport in the same magnitude as the locally generated waves along certain shoreline stretches. The shifting between larger and smaller sediment transport values at the locations along the coast is caused by the relationship between the shoreline orientation and the distribution of the incident wave direction. The calculations are quite sensitive to this relationship; even a one-degree difference in shoreline orientation can cause significant change in sediment transport.

7.2 Wave runup and dune/berm impact

The calculations in this case are based on the profiles collected by SOPAC and Ibaraki University, the calculated wave climate in the lagoon, and the recorded sea levels. The observed eroded material used in the calibration may vary alongshore and the waves that reach the beach may be affected by the reefs and other obstacles. However, the results should give an indication of the relative effects from the possible sea-level rise scenarios since the same basic conditions have been used in all scenarios. It should

be kept in mind that the possible growth of reefs and the natural adjustment of the profile have been neglected in this case. It is well known that a beach profile change shape depending on the forcing conditions, adapting their shape to achieve equilibrium for the particular conditions. This is one of the reasons why only the beach berm has been investigated. On other beaches around the world the berm shift its location frequently, but on Majuro the sediment on the berm is more stable and kept in place by vegetation. However, during severe events (i.e., high waves and water levels), sediment is transported from the berm in spite of the stabilizing influence of the vegetation. Although the present calculations are based on only one profile and the results in principal only can be implemented in the direct vicinity of this profile, several of the documented profiles show more or less the same behavior and qualitatively useful conclusions may be drawn about these profiles as well.

The magnitude of erosion depends on the interaction between the cross-shore and longshore sediment transport. In theory, the cross-shore transport spreads the material across the profile depending on the forcing and the longshore sediment transport move the sediment along the beach. This is a natural ongoing phenomenon that results in shoreline change over time. The conflict often occurs when human activity impacts the natural processes. It is important to keep in mind that the transport and associated gradients not only mean erosion, but the same process occurs when a beach is created by accumulation of sediment.

When looking at the other profiles investigated by SOPAC and Yokoki et al, there are places where accumulation of sediment occurs, but at most profiles the signs of erosion are even greater than in profile 8.

7.3 Sea levels and future scenarios

The future scenarios were chosen to show both the upper and lower range of a possible sea-level rise. The scenarios are not expressed as a prediction of any sort, rather as an indicator of what current climate change studies are showing. Both IPCC and the Delta Committee are highly regarded in their fields, still long-term future prediction holds far too many uncertainties to be taken in full confidence.

The results for the different sea-level rise scenarios applied to Profile 8 show that a complete erosion of the beach profile could occur within 60-90 years. It reflects, however, only one location along the shoreline of Majuro. Profile measurements are limited by the lack of sandy beaches on Majuro; thus, the SOPAC measurements are currently only being performed on Laura where sandy beaches can be found.

7.4 Topography

One of many reasons for coastal erosion is extracting natural resources from the ground. This in combination with a possible sea level rise will change the conditions for erosion at the island extensively. Although it is hard to say which part and in what magnitude the Island will be flooded a simple comparison can be done between the current situation and a worst case scenario of a sea level rise of 0.76 m see Figure 7.1.

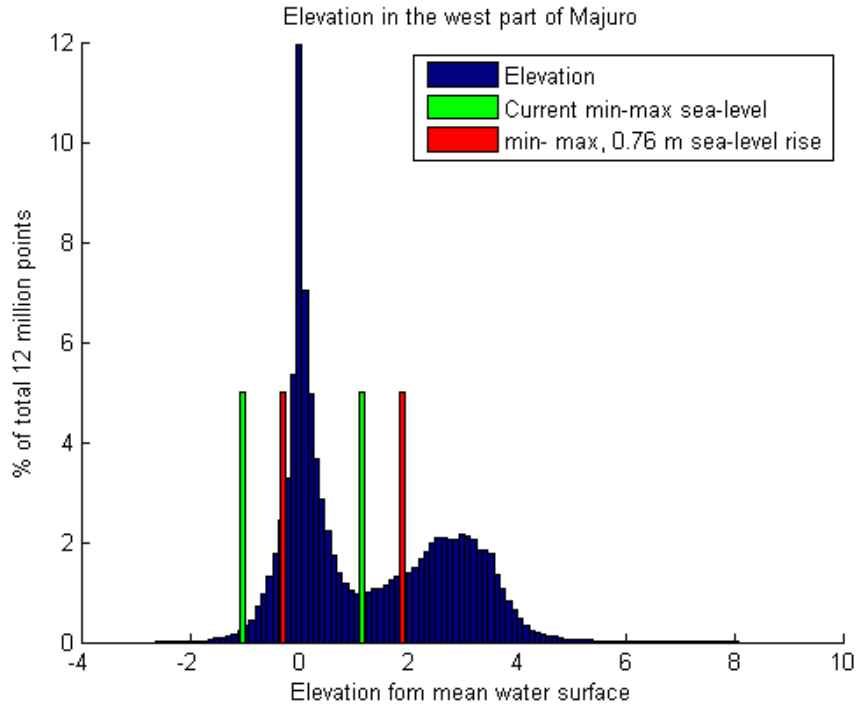


Figure 7.1 Histogram of elevation on the western rim of Majuro together with present and future sea levels.

In the worst case scenario of a sea-level rise of 0.76 m by 2100 and a width of 1250 m and a mean height of 2.7 m, roughly 375 m of the beach would be gone.



Figure 7.2 Possible erosion scenario on Laura.

7.5 Overtopping

The overtopping on Majuro in December 2008 was likely a result of large swell waves created by the low pressure close to Wake Island 500 miles away. However, we do not know if there was any overtopping event during the calibration period, but the calculations should still give an indication of the impact of a possible sea-level rise. Another thing that can change the result of the present analysis is the possible change in storm system characteristics due to climate change.

8 Conclusions

Coastal erosion on Majuro was investigated as early as in the 1970's. Even 40 years ago, researchers warned about poor coastal management and the potential effects of coastal erosion. The reasons for the slow advances on coastal issues on Majuro are likely of combination poverty, high population rate, cultural, and social attitudes. Coastal problems are usually expensive to solve and it may be difficult for a small nation with limited resources. More urgent areas in policy-makers opinions, such as education and health care, might be prioritized. Like many other developing countries, a high population rate is often related to poverty. An environmental awareness program has been launched by the Majuro EPA that focuses on educating the locals on environmental issues such as waste management and coastal problems. Cultural and social difficulties are also connected with poverty and tend to bring individuals further away from a solidarity solution on national matters.

The results from the potential longshore sediment transport calculations on the lagoon side show a transport direction that varies and a magnitude within a wide range from 2500-330 000 m³/y (diffraction and local waves combined), depending on location on the island. However, the sediment transport direction for only locally generated waves agrees well with the results of Xue (2001). According to the results from the transport calculations for diffracted ocean waves, in places where diffraction and local waves interact, diffraction plays a very important role in transporting the sediments. This conclusion is based on the calculations performed in this report as well as the results presented by Yokoki et al. (Yokoki, 2005). Even though the diffraction may be overestimated, it is a major contributor to the sediment movement along Majuro coastlines.

The dune/berm impact from waves in combination with sea-level rise implies increased erosion in all of the three scenarios of a sea-level rise investigated using current wave conditions on Majuro. The time it takes to erode 25m²/m of berm on Laura ranges between 60 and 90 years for all three scenarios. A more distinct difference can be seen during the latter half (2050-2100) of the scenario period. The sediment transport in Scenario 3 with an exponential sea-level rise increases up to five times compared to Scenario 1 and 2 by 2100. IPCC along with many researchers in the coastal science field believe that an exponential increase in the sea-level rise is the most probable course of event. If Scenario 3 is realized, Majuro might not see the full force of the consequences from sea-level rise until it is too late to do anything about it. Thus, Scenario 3 should give an indication of the pressing matter of climate and coastal threats.

Overtopping is also more likely to occur as sea level rises. The problematic with overtopping is how to protect the island based on a cost-benefit analysis. Damages from flooding alone might not motivate investments in preventive infrastructure. Both local and national financial means are limited on Majuro.

Change in attitudes and increasing awareness from different medias has taken climate change and coastal problems to more open forums than ever before. But for an isolated island in a developing country in the Pacific Ocean, change takes much longer time. Many climate and coastal efforts have already been performed on Majuro and more will follow. The most important aspect is try to involve more local people into the movement: Active participation and work towards a solidarity spirit for their homes and for their island.

9 References

Literature Cited

Bayram, A., Larson, M., & Hanson, H. (2007). *A new formula for the total longshore sediment transport rate*. Lund University, Department of Water Resources Engineering, Lund, Sweden.

Beger, M., Jacobson, D., Pinca, S., Richards, T. Z., Hess, D., Page, K., et al. (2008). *"The State of Coral Reef Ecosystems of the Republic of the Marshall Islands" in: The State of Coral Reef Ecosystems of the United States and Pacific Freely Associated States: 2008*. (J. E. Waddell, & A. M. Clarke, Eds.) NOAA.

Bernstein, L., Bosch, P., Canziani, O., Chen, Z., Christ, R., Davidson, O., et al. (2007). *Synthesis Report - An Assessment of the Intergovernmental Panel on Climate Change*. (A. Allali, R. Bojariu, S. Diaz, E. Ismail, D. Griggs, D. Hawkins, et al., Eds.) Geneva, Switzerland: IPCC.

Dalrymple, R. A. (1984). *Water wave mechanics for Engineers and Scientists*. Englewood Cliffs, New Jersey, US: Prentice-Hall, Inc.

Delta Committee. (2008). *Working together with water - A living land builds for its future*. Delta Commissie 2008.

Komar, P. D. (1997). *Beach Processes and Sedimentation* (2nd ed.). Prentice Hall.

Larson, M., Erikson, L., & Hanson, H. (2004). *An analytical model to predict dune erosion due to wave impact*. Department of Water Resources Engineering, Lund Institute of Technology, Lund University, Lund, Sweden.

Larson, M., Kraus, N. C., & Hanson, H. (2002). Simulation of Regional Longshore Sediment Transport and Coastal Evolution - the "Cascade" Model. *Costal Engineering Conference*, (p. 14). World Scientific Press.

Mimura, N., Nurse, L., McLean, R. F., Agard, J., Briguglio, L., Lefale, P., et al. (2007). *Small Islands. Climate Change 2007: Impacts, Adaptation and Vulnerability. Contribution of Working Group II to the Fourth Assessment Report of the Intergovernmental Panel on Climate Change*. (M. L. Perry, O. F. Canziani, J. P. Palutikof, P. J. van der Linden, & C. E. Hanson, Eds.) Cambridge University Press, Cambridge, UK, 687-716.

Nakicenovic, N., Davidson, O., Davis, G., Grübler, A., Kram, T., Lebre La Rovere, E., et al. (2000). *Emission Scenarios - Summary for Policy Makers, A Special Report of IPCC Working Group III of the Intergovernmental Panel of Climate Change*. (N. Nakicenovic, & R. Swart, Eds.) Cambridge, UK: Cambridge University Press.

Soulsby, R. (1998). *Dynamics of Marine Sands*. London: Thomas Telford Ltd.

The National Biodiversity Team of the Republic of the Marshall Islands. (2000). *The Marshall Islands - Living Atolls Amidst the Living Sea*. Santa Clarita: St. Hildegard Publishing Company.

U.S. Army Corps of Engineers. (2002). *Coastal Engineering Manual*. Washington, D.C.

Woodward, P., & Woodward, M. (1998). *Survey of DUD and Laura beach profiles, Majuro Atoll, Republic of Marshall Islands*. SOPAC Preliminary Report 93: Prepared for the Republic of Marshall Islands with Support from the Government of Australia.

Xue, C. (2001). Coastal erosion and management of Majuro Atoll, Marshall Islands. *Journal of Coastal Research*, Vol 17, No 4 , pp909-918.

Yamano, H., Shimazaki, H., Matsunaga, T., Ishoda, A., McClennen, C., Yokoki, H., et al. (2006). Evaluation of various satellite sensors for waterline extraction in a coral reef environment: Majuro Atoll, Marshall Islands. *Geomorphology*, Vol 82, Issue 3-4 , pp398-411.

Yokoki, Y. K. (2005). *Comparison between Longshore Sediment Transport Due to Waves and Long-term Shoreline change in Majuro Atoll, Marshall Islands*. *Global Environmental Research* 9 (1)/2005:21-26.

Online Sources

AusBOM. (2010). *South Pacific Sea Level and Climate Monitoring Project Hourly Sea Level and Meteorological Data*. Retrieved January 28, 2010, from Australian Government, Bureau of Meteorology:

<http://www.bom.gov.au/oceanography/projects/spslcmp/data/index.shtml>

GLOSS. (2008, May 29). *The Global Sea Level Observation System*. Retrieved January 22, 2010, from What is GLOSS?:

<http://www.gloss-sealevel.org/>

Hanson, H. (2010). *Lund Universitet, Faculty of Engineering, LTH*. Retrieved March 22, 2010, from Lectures - Coastal Hydraulics -

VVR040: <http://www.tvrl.lth.se/utbildning/courses/vvr040/lectures/>

IPCC. (2010). *History*. Retrieved March 14, 2010, from IPCC - Intergovernmental Panel on Climate Change:

http://www.ipcc.ch/organization/organization_history.htm

KNMI. (2000). *Royal Netherlands Meteorological Institute, Ministry of Transport, Public Works and Water Management*.

Retrieved January 11, 2010, from The KNMI/ERA-40 WAVE ATLAS:

<http://www.knmi.nl/onderzk/oceano/waves/era40/license.cgi>

MIVA. (2005). *Climate*. Retrieved January 13, 2010, from Marshall Islands Visitors Authority:

<http://www.visitmarshallislands.com/climate.htm>

RMI Embassy. (2008). *General Information*. Retrieved January 13, 2010, from Embassy of the Republic of the Marshall Islands:

<http://www.rmiembassyus.org/General%20Info.htm#overview>

RMI Embassy. (2008). *History*. Retrieved January 13, 2010, from Embassy of the Republic of the Marshall Islands:

<http://www.rmiembassyus.org/History.htm>

SMHI. (2009). *El Niño och La Niña, Oceanografi, Kunskapsbanken*. Retrieved March 14, 2010, from SMHI - Swedish Meteorological and Hydrological Institute: <http://www.smhi.se/kunskapsbanken/oceanografi/el-ni-o-och-la-ni-a-1.7053>

SOPAC. (1995). *Sand and Aggregate Resources Majuro Atoll, Marshall Islands, SOPAC Technical Report 215*. Retrieved January 15, 2010, from <http://map.sopac.org/data/virlib/TR/TR0215.pdf>

SPSLCP. (2007, December). *South Pacific Island Reports: Marshall Islands*. Retrieved January 22, 2010, from South Pacific Sea Level and Climate Monitoring Project: <http://www.bom.gov.au/ntc/IDO60024/IDO60024.2007.pdf>

Appendix I – Abbreviations

Abbreviation	Explanation
AR4	IPCC's Fourth Assessment Report
AusBom	Australian Government Bureau of Meteorology
AusAid	The Australian Government's Overseas Aid Program
DUD	Islets Darit, Uliga and Dalap on Majuro Atoll (Majuro town center)
EPA	Environmental Protection Authority
GLOSS	Global Sea Level Observation System
IOC	Intergovernmental Oceanographic Commission
IPCC	Intergovernmental Panel on Climate Change
JCOMM	Joint Commission for Oceanography and Marine Meteorology
KMNI	Royal Netherlands Meteorological Institute
LST	Longshore Sediment Transport
MIVA	Marshall Islands Visitors Authority
OECD	Organization for Economic Co-operation and Development
RMI	Republic of the Marshall Islands
SEAFRAME	Sea Level Fine Resolution Acoustic Measuring Equipment
SIDA	Swedish International Development Cooperation Agency
SMHI	Swedish Meteorological and Hydrological Institute
SOPAC	Pacific Islands Applied Geoscience Commission
SPSLCP	South Pacific Sea Level and Climate Project
SRES	IPCC' Special Report Emission Scenarios
UNFCCC	United Nations Framework Convention on Climate Change
WMO	World Meteorological Organization

Appendix II – Computing wave climate in the lagoon from wind data

Because of lacking information, the wind data from the SEAFRAME station at Majuro are assumed to be measured at 10 meter elevation. To be able to use the wind speed (U) in wave growth formulas, the wind speed must first be expressed in terms of wind-stress factor U_A (adjusted wind speed). (U.S. Army Corps of Engineers, 2002)

$$U_A = 0.71 \cdot U^{1.23} \quad (\text{II-1})$$

The fetch length in the Majuro lagoon is assumed to be the limiting factor because of their short lengths. Under fetch-limited conditions winds have blown constantly long enough for wave heights at the end of the fetch to reach equilibrium. Combining the fetch lengths (F) for each point along the coast line (Figure 4.16 and Figure 4.17) with the adjusted wind speed that occurs in the fetch direction, a wave height (H_s), wave period (T_m) and wind duration (T) can be obtained under fetch.limited conditions. (U.S. Army Corps of Engineers, 2002):

$$H_s = 1.613 \cdot 10^{-2} \cdot U_A \cdot F^{\frac{1}{2}} \quad (\text{II-2})$$

$$T_m = 6.238 \cdot 10^{-1} \cdot U_A \cdot F^{\frac{1}{3}} \quad (\text{II-3})$$

$$T = 8.93 \cdot 10^{-1} \cdot \left(\frac{F^2}{U_A} \right)^{\frac{1}{3}} \quad (\text{II-4})$$

Appendix III – Calculations of longshore sediment transport rate

Variable	Symbol	Assumed values
Density water	ρ	1025 (kg/m ³)
Density Solid	ρ_s	2264 (kg/m ³)
Gravity	g	9.8 (m/s ²)
Kinematic viscosity at 28C°	ν	0.08847·10 ⁻⁶ (m ² /s)
Median grain size	d_{50}	0.00025 m
Bottom friction coefficient	c_f	0.005
Porosity	a	0.4
Breaking wave index	γ_b	0.78

$$Q_{lst} = \frac{\varepsilon}{(\rho_s - \rho)(1 - a)gw_s} F\bar{V} \quad (III-1)$$

Q_{lst} is the longshore sediment transport rate in volume per unit time, ε is the empirical transport coefficient describing waves efficiency of keeping sand grains in suspension (Larson, Kraus & Hanson, 2002) given by:

$$\varepsilon = 0.77 \cdot c_f \cdot K \quad (III-2)$$

where c_f is the bottom friction coefficient set to 0.005 and K is an empirical coefficient from the CERC formula set to 0.2. ρ_s and ρ is solid density of the sediment and the water density, respectively, the porosity is given as a and is set to 0.4, g is the acceleration due to gravity, w_s is sediment fall speed (Soulsby, 1998) given by:

$$w_s = \left(\frac{\nu}{d_{50}}\right) \cdot \left[(10.36^2 + 1.049D^*)^{\frac{1}{2}} - 10.39 \right] \quad (III-3)$$

ν is the kinematic viscosity at the average water temperature (Soulsby, 1998), d_{50} is median grain size of the sediment and D^* is the dimensionless grain size (Soulsby, 1998) given by:

$$D^* = \left[\frac{g(s-1)}{\nu} \right]^{\frac{1}{3}} \cdot d_{50} \quad (III-4)$$

where s is the ration of densities of grain and water and d is the median sieve diameter of grains. F in the Q_{lst} equation is the wave energy flux given by:

$$F = \frac{1}{8} \delta g H_b^2 C_g \cdot \cos \theta_b \quad (\text{III-5})$$

δ is the water density at the average water temperature, H_b is the breaking wave height and θ_b the breaking wave angle (Larson, Kraus & Hanson, 2002) given by:

$$\theta_b = \arcsin \left(\sqrt{2\pi} \cdot \sin \theta_b \sqrt{\frac{H_b}{L_0}} \right) \quad (\text{III-6})$$

and C_g is the individual wave group velocity for each wave given by:

$$C_g = \frac{L_0}{2 \cdot tm} \quad (\text{III-7})$$

where L_0 is the wave length in deep waters and tm is the wave period for each individual wave. \bar{V} in the Q_{ist} equation is the mean longshore current velocity over the surf zone given by:

$$\bar{V} = \frac{5}{32} \cdot \frac{\pi \gamma_b \sqrt{g}}{c_f} A^3 \cdot \sin \theta_b \quad (\text{III-8})$$

where γ_b is the breaker index set to 0.78 and A is the shape parameter (Soulsby, 1998) given by:

$$A = 2.25 \left(\frac{W_b^2}{g} \right)^{\frac{1}{3}} \quad (\text{III-9})$$

To find a breaking wave height H_b , a formula from Larson, Kraus & Hanson, 2002, was adapted using the deepwater wave length L_0 , wave height to water depth atincipent breaking γ_b and deepwater wave angle in respect to the shoreline orientation θ_b .

$$L_0 = 1.56 \cdot tm^2 \quad (\text{III-10})$$

$$h_b = \left(\frac{h}{L_0} \right)^2 \cdot \left(\frac{\cos \theta_b}{0.78 \cdot 2 \cdot \sqrt{2\pi}} \right)^{\frac{2}{5}} \cdot L_0 \quad (\text{III-11})$$

The breaking wave height is then used to calculate the longshore sediment transport.

Appendix IV – Profiles at Laura

The following beach profiles were measured by SOPAC (Woodward & Woodward, 1998) and the follow-ups has been done by Professor Yokoki, et al., Ibaraki University.

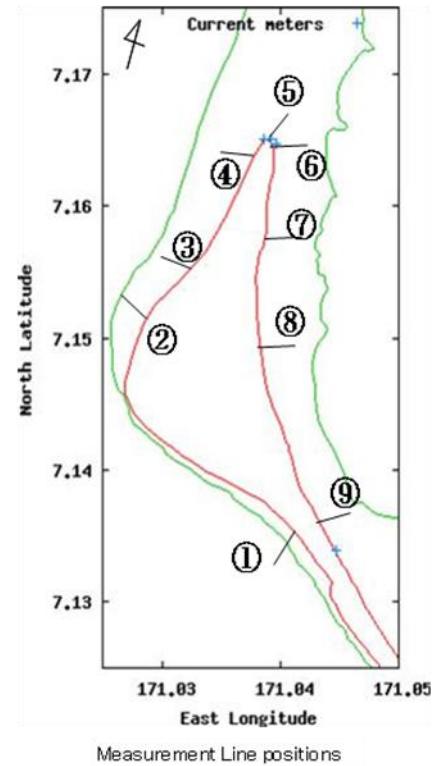


Figure IV.1 SOCAP and Yokoki profile measurements on Laura.

Profile 1

According to SOPAC there were no visible changes between 1997 and 1998. No follow-up has been done.

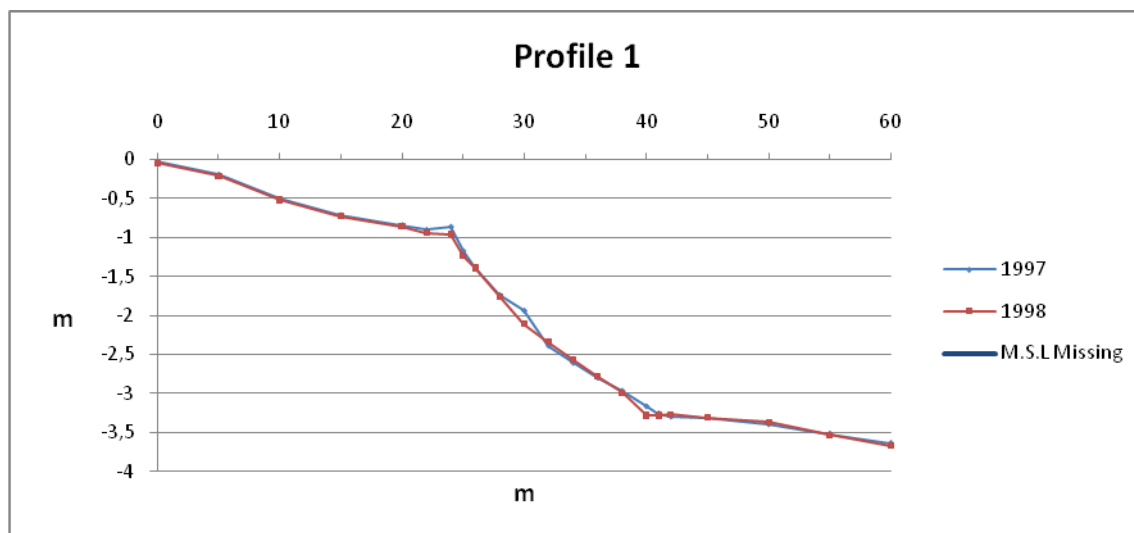


Figure IV.2 Beach Profile 1 on Laura.

Profile 2

According to SOPAC there appeared to be some movement of the sediment at 20 – 34 m between 1997 and 1998. No follow-up has been done.

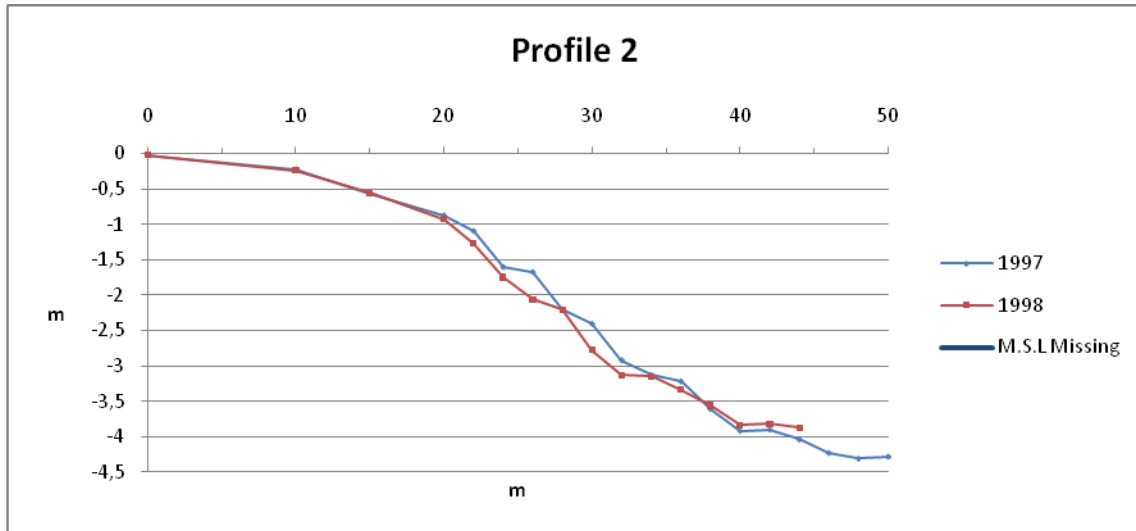


Figure IV.3 Beach Profile 2 on Laura.

Profile 3

According to SOPAC there were small changes in the profile and some changes in the beach scarp between 1997 and 1998. Between the years 2006 – 2009 follow-ups were done by Ibaraki University, comparing the profiles done by SOPAC and Ibaraki University there was accumulation between the years 1998 and 2006 and then erosion back to its former state between 2006 - 2009.

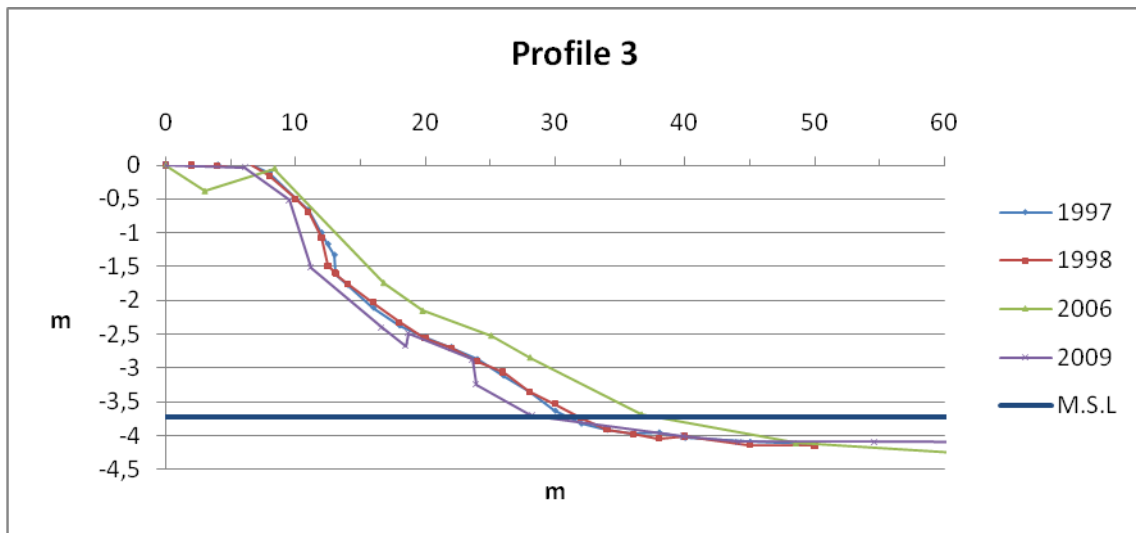


Figure IV.4 Beach Profile 3 on Laura.

Profile 4

According to SOPAC the scarp had moved 6 m inland between 1997 and 1998. In the follow-ups done by Ibaraki University, the beach scarp has accumulated about 12 m since 1997.

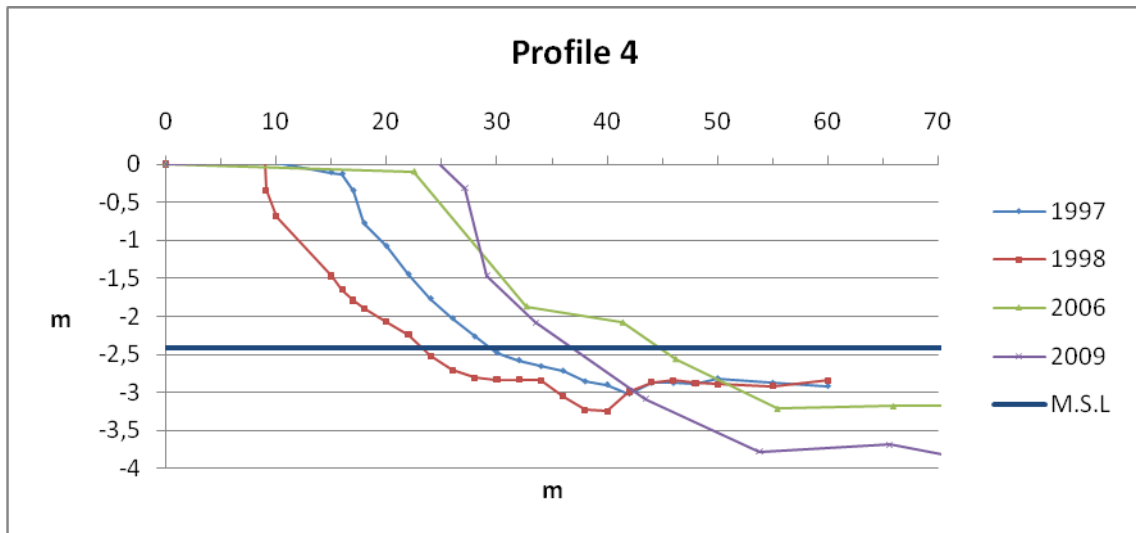


Figure IV.5 Beach Profile 4 on Laura.

Profile 5

According to SOPAC the scarp had moved 10 m inland between 1997 and 1998. In the follow-ups done by Ibaraki University, the scarp has continued to withdraw. In 2009 the scarp had continued to move approximately 30 m since 1998.

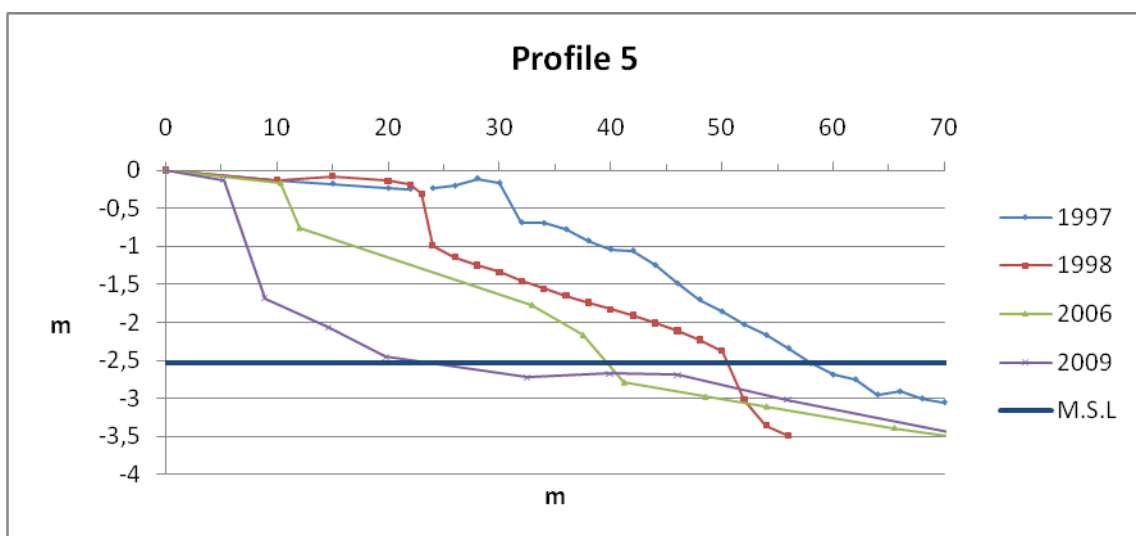


Figure IV.6 Beach Profile 5 on Laura.

Profile 6

According to SOPAC there was extensive accumulation of approximately 30 between 1997 and 1998. In the follow-ups done by Ibaraki University, the beach has eroded back approximately 50 m since 1998, but there seems to be some accumulation of the scarp.

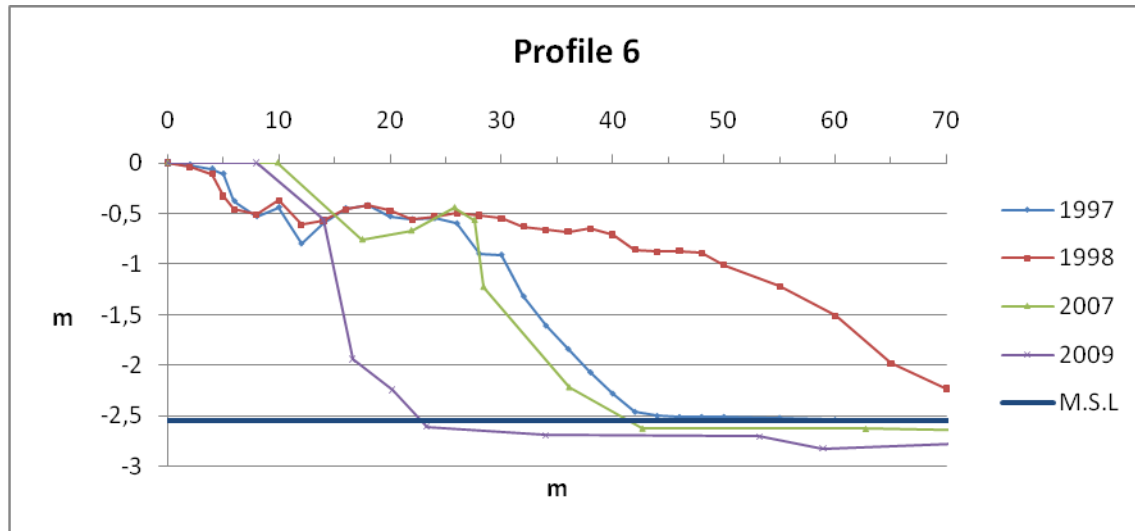


Figure IV.7 Beach Profile 6 on Laura.

Profile 7

According to SOPAC there was some erosion of the scarp of approximately 2 m and some accumulation of sediment on the beach between 1997 and 1998. In the follow-ups done by Ibaraki University, both the scarp and the beach have eroded.

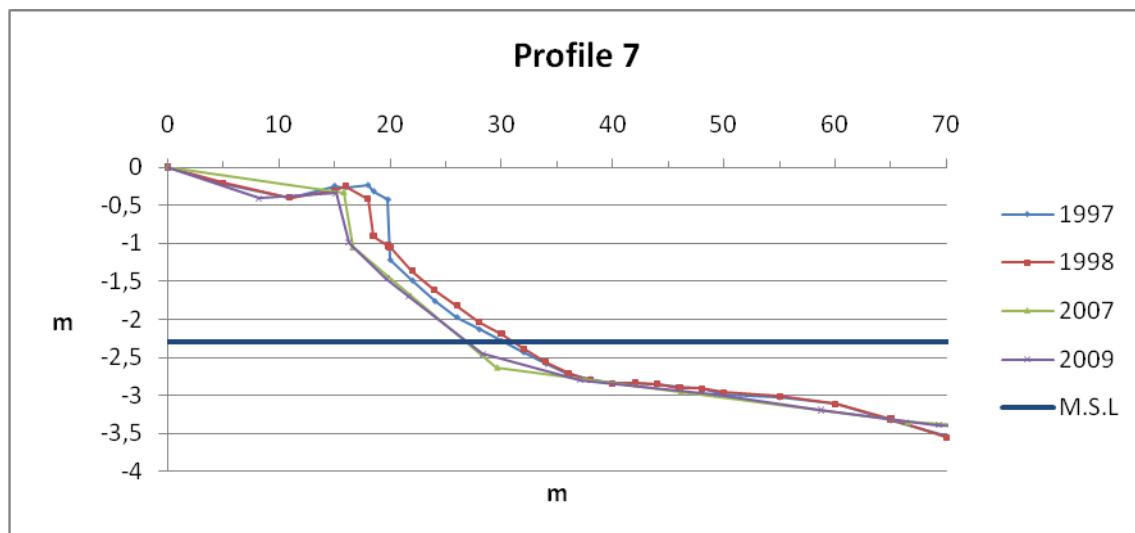


Figure IV.8 Beach Profile 7 on Laura.

Profile 8

According to SOPAC there were small erosion of the scarp in the magnitude of 0.3 m and some erosion on the beach between 1997 and 1998. In the follow-ups done by Ibaraki University, comparing the profiles done by SOPAC and Ibaraki University there was accumulation on the lower part of the beach between the years 1998 and 2006 and then the beach eroded between 2006 and 2009. The scarp has continued to erode a total of approximately 2 m from 1997 – 2009.

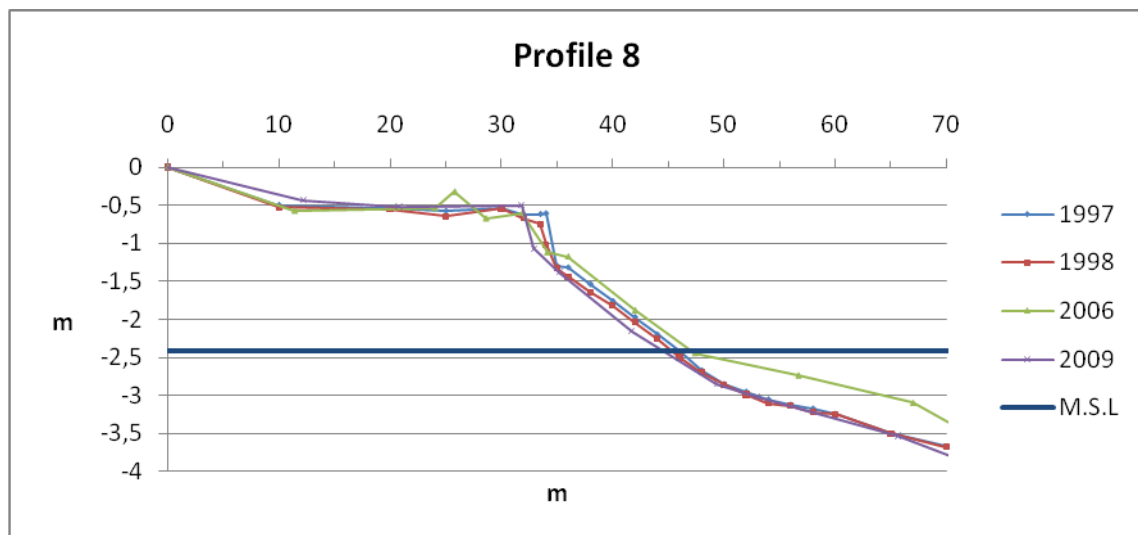


Figure IV.9 Beach Profile 8 on Laura.

Profile 9

According to SOPAC erosion was noted along the profile between 1997 and 1998. No follow-up has been done.

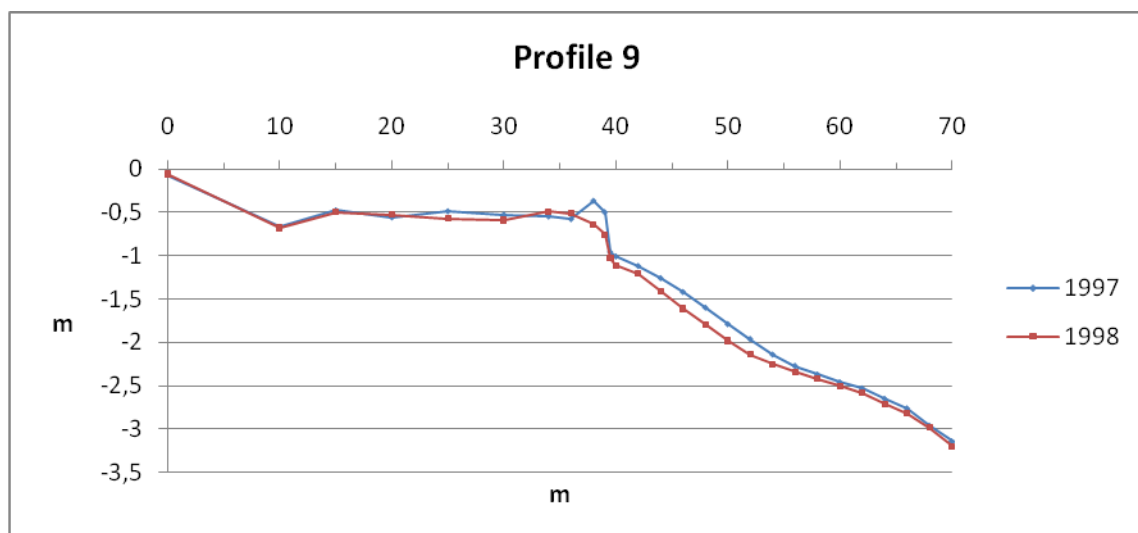


Figure IV.10 Beach Profile 9 on Laura.

Appendix V – Wind distribution at Majuro, Marshall Islands (GLOSS)

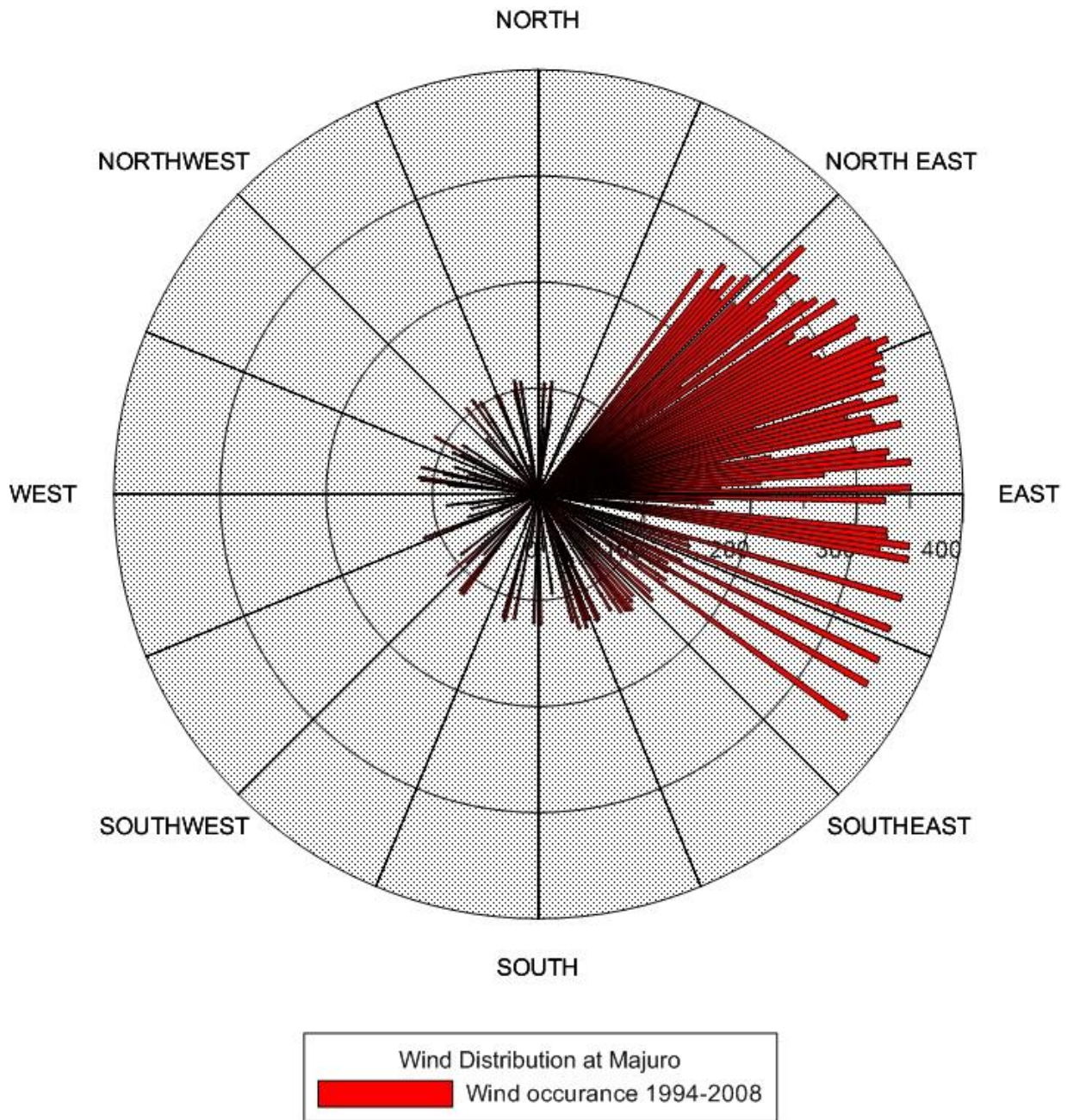


Figure V.1 Wind distribution on Majuro

Appendix VII – Sediment transport as a result of diffraction

22.5° wave angle approach

Table VII.1 22.5° wave angle approach for two cases

Diffraction in lagoon	east to west		Sediment transport Q L ₀ = 90.87, T = 8, depth = 4m	
	k'	m	H = 1.42, 4.53% of all waves	H=1.6, 13.47% of all waves
1	0.2	0	-3894	-14699
2	0.3	1000	-6408	-24190
3	0.4	3000	-3856	-14556
4	0.7	4000	-13766	-51967
5	0.7	5000	3943	14885
6	0.7	6000	-7881	-29750
7	0.7	7000	34866	131607
8	0.6	8000	2897	10936
9	0.7	9000	15719	59342
10	0.5	10000	3017	11388
11	0.4	11000	22126	83498
12	0.3	12000	9084	34289
13	0.2	13000	6156	23233
sum			62003	234016

60° wave angle approach

Table VII.2 60° wave angle approach

Diffraction in lagoon	east to west		Sediment transport Q L ₀ = 76.44, T = 7, depth = 2m
	k'	m	H = 0.8, 25.3% of all waves
1	0.2	0	9445
2	0.3	1000	32127
3	0.4	2000	58838
4	0.5	3000	82746
5	0.5	4000	65483
6	0.4	5000	27525
7	0.3	6000	12665
8	0.2	7000	5115
9	0.2	8000	-1643
Sum			292301

Appendix VIII – Erosion scenarios with regard to sea-level rise

Erosion calculations are based on sea level data on Majuro from 1999-2008 and each 10-year period consist of 87460 hourly measurements.

Scenario 1

Table VIII.1 Erosion for 0.25 m sea-level rise m in 100 years based on 87460 h/10 years of

S.L.R 0.25 m in 100 years				
Year and tot S.L.R	time (%)	Sea levels above z_0	sum (m³)/decade	sum tot(m³)
jan 1999- dec 2008	0,28	247	0,7	
jan 2009-dec 2018 +0.025 m	0,37	324	1,0	1,7
jan 2019-dec 2028 +0.050 m	0,49	431	1,3	3,0
jan 2029-dec 2038 +0.075 m	0,64	558	1,8	4,8
jan 2039-dec 2048 +0.100 m	0,80	703	2,4	7,2
jan 2049-dec 2058 +0.125 m	0,99	863	3,3	10,5
jan 2059-dec 2068 +0.150 m	1,23	1079	4,4	15,0
jan 2069-dec 2078 +0.175 m	1,50	1313	6,0	21,0
jan 2079-dec 2088 +0.200 m	1,81	1581	8,0	28,9
jan 2089-dec 2098 +0.225 m	2,14	1873	10,4	39,3
jan 2099-dec 2108+ 0.250 m	2,51	2195	13,6	52,9

Scenario 2

S.L.R 0.44 m in 100 years				
Year and tot S.L.R	time (%)	time (h) / tot 87460 h	sum (m³)/decade	sum tot(m³)
jan 1999- dec 2008	0,28	247	0,7	
jan 2009-dec 2018 +0.044 m	0,47	407	1,2	2,0
jan 2019-dec 2028 +0.088 m	0,72	628	2,1	4,1
jan 2029-dec 2038 +0.132 m	1,06	927	3,6	7,6
jan 2039-dec 2048 +0.176 m	1,51	1322	6,0	13,7
jan 2049-dec 2058 +0.220 m	2,08	1819	9,9	23,5
jan 2059-dec 2068 +0.264 m	2,76	2417	15,7	39,2
jan 2069-dec 2078 +0.308 m	3,56	3114	24,2	63,4
jan 2079-dec 2088 +0.352 m	4,51	3943	36,2	99,6
jan 2089-dec 2098 +.0396 m	5,56	4862	52,6	152,2
jan 2099-dec 2108 +0.440 m	6,77	5922	74,7	227,0

Scenario 3

S.L.R 0.76 m in 100 years				
Year and tot S.L.R	time (%)	time (h) / tot 87460 h	sum (m³)/decade	sum tot(m³)
jan 1999- dec 2008	0,28	247	0,7	
jan 2009-dec 2018 +0.030 m	0,40	352	1,0	1,8
jan 2019-dec 2028 +0.068 m	0,59	520	1,6	3,4

jan 2029-dec 2038 +0.113 m	0,90	791	2,9	6,3
jan 2039-dec 2048 +0.169 m	1,43	1251	5,5	11,8
jan 2049-dec 2058 +0.235 m	2,25	1970	11,6	23,4
jan 2059-dec 2068 +0.313 m	3,68	3216	25,4	48,8
jan 2069-dec 2078 +0.405 m	5,80	5072	56,5	105,3
jan 2079-dec 2088 +0.510 m	9,02	7890	125,4	230,7
jan 2089-dec 2098 +0.632 m	13,54	11842	274,4	505,1
jan 2099-dec 2108 +0.770 m	20,02	17505	584,2	1089,3

Appendix IX – Tabular significant wave height and mean wave period

Tabular significant wave height (corrected ERA-40) and mean wave period bivariate histograms for Lon: 171-180, Lat: 09N-00N, from 1971/01 to 2000/12 (KNMI, 2000).

Dir: 0.- 45.

Total of: 287032 observations, 18.8%

Tm \ Hs	0- 1	1- 2	2- 3	3- 4	4- 5	5- 6	sum
0 - 3	0	0	0	0	0	0	0
3 - 4	0	0	0	0	0	0	0
4 - 5	0	0	0	0	0	0	0
5 - 6	0	43	114	0	0	0	158
6 - 7	0	318	1387	321	6	0	2032
7 - 8	0	997	2043	468	34	0	3542
8 - 9	0	1074	1974	169	18	0	3235
9 - 10	0	82	813	78	1	0	975
10 - 11	0	0	27	30	1	0	57
11 - 12	0	0	0	0	0	0	0
12 - 13	0	0	0	0	0	0	0
13 - 33	0	0	0	0	0	0	0
sum	0	2515	6358	1067	60	0	10000

Dir: 45- 90

Total of: 598286 observations, 38%

Tm \ Hs	0- 1	1- 2	2- 3	3- 4	4- 5	5- 6	sum
0 - 3	0	0	0	0	0	0	0
3 - 4	0	0	0	0	0	0	0
4 - 5	0	6	0	0	0	0	6
5 - 6	0	525	883	3	0	0	1411
6 - 7	0	1292	2425	372	11	0	4100
7 - 8	0	1929	942	113	18	0	3002
8 - 9	0	861	501	10	0	0	1372
9 - 10	0	26	76	5	0	0	108
10 - 11	0	0	1	0	0	0	1
11 - 12	0	0	0	0	0	0	0
12 - 13	0	0	0	0	0	0	0
13 - 33	0	0	0	0	0	0	0
sum	0	4639	4828	503	30	0	10000

Appendix X – Summary of KMNI total waves and significant wave heights at Majuro

Data was collected during 1971-2000

Dir: All

Total of: 1577952 observations, 100%

Tm \ Hs	0- 1	1- 2	2- 3	3- 4	4- 5	5- 6	sum
0 - 3	0	0	0	0	0	0	0
3 - 4	0	0	0	0	0	0	0
4 - 5	0	5	0	0	0	0	5
5 - 6	0	446	399	1	0	0	846
6 - 7	1	1323	1317	201	5	0	2847
7 - 8	1	2858	865	131	13	0	3868
8 - 9	0	1274	741	43	4	0	2061
9 - 10	0	49	262	31	1	0	343
10 - 11	0	0	15	16	0	0	31
11 - 12	0	0	0	0	0	0	0
12 - 13	0	0	0	0	0	0	0
13 - 33	0	0	0	0	0	0	0
sum	2	5954	3598	422	23	0	10000

Appendix XI – Interviews on Majuro and Jaluit

Short interviews were performed on Majuro and Jaluit to find out what people thought about sea-level rise and coastal erosion on their islands. 21 locals were interviewed, both men and women with ages ranging from 21-62. Most of the interviewees were living either close or at the beach line and were chosen randomly.

Majuro

A majority of the interviewees from Majuro had lived their whole life on the island. They all unanimously agree that the beach is getting smaller. Their statements were based on having experienced signs such as falling coconut trees, less sand, more exposed reefs and higher water levels. When asked what they thought could be the reason for the beach getting smaller, some said the expansion and construction of the airport was the cause, which is located on the thinner southern rim of the island. Others mentioned the construction of a causeway located in the southern rim as well, general constructions along the coastline, dredging in the downtown area, climate change and global warming. Most of the interviewees started to notice the changes about 3-6 years ago. Some answered more ambiguously that the changes started in the 70's or when companies started to import products. When asked if there were any other changes along the coast, they most commonly answered that there were a lot less fish in the near coast area and also more trash and dirty waters.

On questions regarding changes in climate, all the interviewees answered that they had experienced some kind of change, for example the warm days were getting hotter, longer periods of droughts and a shifting of seasons, meaning the windy season and the summer season were overlapping more frequently. It was explained that the season shift was most notable by the breadfruit maturing much later than before.

When asked if they have seen or experienced waves washing in over land, a majority answered no. Only a few remembered the overtopping at DUD in December 2008 and only one out of the Majuro locals had ever experienced more than one overtopping.

Finally, the interviewees were asked that they thought about their future and the future of the island. There was mixed answers, some more hopeful and believed in a better future, some less hopeful who believed conditions would become much worse. The people with big families and poor conditions were often more worried about their children and houses. One of the more optimistic answers was that modern technology would improve conditions on the island. How do you think Majuro would look like in 50 years, was the last question and most of the interviewees answered that they didn't know. Some answered that the island would be gone by then. When asked what he will do if that happens, Orlando, 21, answered, "If it (the island) disappears I'll go away on my boat".

Jaluit

The local EPA (Environment Protection Authority) on Majuro sponsored a five day field visit on Jaluit, an atoll 200 km southwest of Majuro. The atoll is almost twice the size of Majuro but much less developed and has only about 1 700 inhabitants.

They too had experienced loss of sandy beaches and falling coconut trees. Alfonso, 48, science teacher, explained that 4-5 lines of coconut trees had fallen into the sea, and that there used to be a cemetery at Jaluit Jaluit, the main islet on Jaluit, that was now under water. He believed that the causes for the change could have something to do with the increasing constructions of seawalls and a change in currents and tides. The changes started 2 years ago according to Alfonso. Other changes that were noticed on the island was higher and lower tides than before, hotter days, heavier rain and change of wind direction. Alfonso's main concerns about the future were increasing population growth, climate change and seawalls being built without proper knowledge.